CHARACTERIZATION OF NLRP13 IN INFLAMMASOME ACTIVITY

by

Mustafa Yalçınkaya

B.S., Molecular Biology and Genetics, Boğaziçi University, 2012

Submitted to the Institute for Graduate Studies in
Science and Engineering in partial fulfillment of
the requirements for the degree of
Master of Science

Graduate Program in Molecular Biology and Genetics
Boğaziçi University
2015

ACKNOWLEDGEMENTS

I would like to thank my supervisor Prof. Nesrin Özören for her supervision and guidance. She always helped and supported me for my project during three years. I am thankful to my thesis committee members Assoc. Prof. Batu Erman and Assoc. Prof. Arzu Çelik for dedicating their time to evaluate my thesis.

I am thankful to Yetiş Gültekin M. Sc., who worked on NLRP13 project during his master thesis before me for his huge effort in this project. His previous results lead the way during my studies and it was a motivating opportunity to have important plasmid constructs that were prepared by him when starting the project. Also, I want to thank specially Aybüke Garipcan M. Sc., for her friendship and great work partnership during my master period in which Aybüke kept my motivation at high level even in hard times and the brainstorming and cooperative work relationship between us was very valuable for me.

I also want to thank to Elif Eren M. Sc., Alican Sahillioğlu M. Sc., Serkan Uğurlu Ph. D., and Duygu Demiröz M. Sc., for their help and guidance, since I learned many techniques and theoretical knowledge from these special labmates. I also appreciate my labmates Ceren Saygı M. Sc., Hulusi Onur Kuzucu and Seda Yasa.

Special thanks to Ekin Ece Erkan M. Sc, Emirhan Taşöz, İzzet Akiva M. Sc., Mahmutcan Hız M. Sc., Burcu Ersoy M. Sc, Ahmet Bugra Tufan M. Sc, Ayşin Demirkol M. Sc., İsmail Tugberk Kaya, Ali İşbilir, Yusuf Enes Kazcı M. Sc., Aslı Uğurlu and Neslihan Zöhrap Ph. D for being my friends and all the previous and current Genreg, Retina and CSL lab members for always sharing their equipments with me during my experiments.

I am also grateful to Çagatay Güvendik, Umut Ünal, Sibel Pehlivan, and my friends for their endless friendliness.

Also, I am indebted to my family for supporting me under all circumstances and in every decision I have made.

Finally, I am thankful to TUBITAK-BIDEB for financing me with BIDEB 2210 Scholarship program during my master period. This work was supported by TUBITAK 112S115 project.

ABSTRACT

CHARACTERIZATION OF NLRP13 IN INFLAMMASOME ACTIVITY

NOD-like receptors (NLRs) are a family of cytoplasmic proteins with members regulating inflammation and apoptosis. NLRP13 is a novel PYRIN domain containing NLR family member and the roles of NLRP13 in these pathways is still unknown. In current literature, there is no paper about NLRP13. NLRP13 expression is very high in oocytes and NLRP13 expression decreases sharply at blastocyst stage. We have previously shown that NLRP13 is mainly localized in the cytoplasm and partially in mitochondria (% 35) using confocal microscopy experiments. Also, we have shown that NLRP13 weakly interacts with inflammatory proteins ASC and Caspase-1 and an inflammasome-like structure between ASC-Caspase-1 and NLRP13 formed under overexpression conditions. In this thesis, we further characterized NLRP13 by trying to figure out its roles in inflammasome activity and immune regulation mechanisms. Firstly, we show that NRLP13 is recruited to ASC specks that formed after LPS and ATP treatment. Secondly, we show that NLRP13 expression decreases upon LPS priming and that ATP is the most potent second signal of NLRP13 inflammasome. Thirdly, we show that NLRP13 increases levels of inflammatory cytokine secretion. NLRP13 polyclonal and monoclonal antibodies were produced and mass spectrometry analysis was done using these antibodies to find the interaction partners of NLRP13. In addition, it can be said that NLRP13 leads to differentiation of monocytes into more M1 macrophage subgroup. Finally, NLRP13 may have roles in the regulation of inflammation at maternal-fetus interface during pregnancy.

ÖZET

NLRP13'ÜN ENFLAMASYON AKTİVASYONUNDAKİ ROLÜNÜN TANIMLANMASI

NOD benzeri alıcılar enflamasyon ve apoptozu düzenleyen sitoplazmik protein ailesinin üyeleridir. NLRP13 PYRIN bölgesi içeren NLR aile üyesidir ve enflamasyon ile apoptozdaki görevleri bilinmemektedir. Literatürde henüz NLRP13 ile ilgili hiçbir yayın bulunmamaktadır. NLRP13 ifadesi olgunlaşmamış yumurtalarda oldukça yüksektir ve NLRP13 ifadesi blastosit döneminde aniden düşmektedir. Yakın zamanda bizim laboratuvarda, NLRP13'ün sitoplazma ve az da olsa mitokondride (% 35) bulunduğunu mikroskop deneylerinde göstermiştirişti. Ayrıca, NLRP13'ün enflamasyon proteinleri Caspase-1 ve ASC ile etkileştigi ve NLRP13'ün, ASC ve Caspase-1 ile enflamazom benzeri yapılar yaptıgı aşırı ifade koşullarında gösterilmiştir. Bu tezde, NLRP13 enflamazom aktivitesi ve bagışıklık düzenleyici mekanizmalarındaki görevleri daha ayrıntılı ortaya çıkarılmaya çalışıldı. İlk olarak NLRP13'ün, hücrelerin LPS ve ATP ile uyarılmasıyla oluşan ASC zerrelerinin yapısına katıldığı gösterilmiştir. İkinci olarak, NLRP13 ifadesi LPS ile uyarılması sonucu düşmektüğü ve ATP'nin NLRP13 enflamazomun potansiyel ikinci sinyali olabilecegi gösterildi. Üçüncü olarak, NLRP13'ün enflamasyon yapıcı sitokin salınımları seviyelerini artırdığı gösterildi. Poliklonal ve monoklonal NLRP13 antikorları üretildi ve bu antikorlar kullanılarak NLRP13 ile etkileşen proteinleri bulmak için kütle specktrometrisi analizleri yapıldı. Bunlara ilaveten, NLRP13'ün monositlerin M1 makrofajlarına dönüşümünü teşvik ettiği söylenebilir. Son olarak, NLRP13'nin hamilelik sırasındaki anne-fetus etkileşimi için gerekli olan enflamasyonun regulasyonunda görevi olabileceği gösterilmiştir.

TABLE OF CONTENTS

LIST OF FIGURES

LIST OF TABLES

LIST OF SYMBOLS

g	Gravity
gr	Gram
kb	Kilobase
kDa	Kilodalton
L	Liter
M	Molar
mg	Milligram
min	Minute
ml	Milliliter
mm	Millimeter
mM	Millimolar
ng	Nanogram
^{o}C	Centigrade degree
sec	Second
V	Volt
µg	Microgram
µl	Microliter
α	Alpha
β	Beta
γ	Gamma
κ	Kappa

LIST OF ACRONYMS / ABBREVIATIONS

APC	Antigen Presenting Cell
APS	Ammonium Persulfate
ASC	Apoptosis Associated Speck-Like Protein Containing CARD
BIR	Baculovirus Inhibitor Repeat
BSA	Bovine Serum Albumin
CARD	Caspase Recruitment Domain
Caspase	Cysteine-Aspartic Proteases
CBB	Commassie Brilliant Blue
cDNA	Complementary DNA
CFP	Cyan Fluorescent Protein
CO2	Carbondioxide
DAMP	Danger-Associated-Molecular-Patterns
DC	Dendritic Cell
DMEM	Dulbecco's Modified Eagle Medium
DMSO	Dimethyl Sulfoxide
DNA	Deoxyribonucleic Acid
dsDNA	Double Stranded DNA
dsRNA	Double Stranded RNA
EDTA	Ethylenediaminetetraacetic Acid
EGFP	Enhanced Green Fluorescent Protein
ER	Endoplasmic Reticulum
FasL	Fas Ligand
FBS	Fetal Bovine Serum
GFP	Green Fluorescent Protein
H_2O	Water
HBS	HEPES Balanced Salt
HEK	Human Embryonic Kidney
HLA	Human Leukocyte Antigen
IFN	Interferon

IgG	Immunoglobulin G
IL	Interleukin
IL1R	IL1 Receptor
IL-1β	Interleukin 1- beta
IP	Immunoprecipitation
LB	Luria-Bertani Broth
LPS	Lipopolysaccaride
LRR	Leucin Rich Repeat
MDP	Muramyl Dipeptide
$MgCl_2$	Magnesium Chloride
MHC	Major Histocompatibility Complex
mRNA	Messanger RNA
mt	Mutant
NACHT	Domain Present in NAIP, CIITA, HET-E, TP-1
NaCl	Sodium Chloride
NAD	NACHT-associated Domain
NBD	Nucleotide Binding Domain
NEAA	Non-esential Amino acid
NF-κB	Nuclear Factor kappa B
NK	Natural Killer
NLR	NOD-Like Receptor
NLRP	NBD, LRR and PYD Containing Proteins
NOD	Nucleotide-Binding Oligomerization Domain
OD	Optic Density
ORF	Open Reading Frame
PAMP	Pathogen-Associated Molecular Pattern
PBS	Phosphate Buffered Saline
PCR	Polymerase Chain Reaction
Pen/Strep	Penicillin/Streptomycin
PRR	Pattern Recognition Receptor
PYD	PYRIN Domain
RPM	Rotations per Minute
RT-PCR	Reverse Transcriptase Polymerase Chain Reaction

SDS	Sodium Dedocyl Sulfate
SDS-PAGE	SDS- Polyacrylamide Gel Electrophoresis
shRNA	Short Hairpin RNA
TAE	Tris-Acetate-EDTA
TBS	Tris Buffered Saline
TBST	Tris Buffered Saline Tween
TEMED	N,N,N’,N’-Tetramethylethane-1,2-diamine
TGF	Transforming Growth Factor
TIR domain	Toll/IL-1 Receptor Domain
TLR	Toll-Like Receptor
TNF	Tumor Necrosis Factor
TRAF	TNF Receptor Associated Factor
Tween	Polysorbate
v	Volume
w	Weight
WB	Western Blot
WT	Wild-Type

1. INTRODUCTION

1.1. Innate Immune System

In humans, there are two parts of defense systems: innate immunity and adaptive immunity. The former is first line of our immune system, also known as the nonspecific immune system and cooperation of these two parts of immunity is required for complete removal of the invading pathogens.

When any pathogen enters the body, the barriers of the innate immune system are the first obstacles to face the pathogenic invasion. These barriers are physical barriers, chemicals and biological barriers. Physical barriers such as the skin, epithelial sheets of gastrointestinal tract, respiratory track and chemicals like antimicrobial peptides, stomach acid, and saliva are nonspecific to any pathogens and block the entrance and spreading of the pathogens. The biological barriers of innate immunity consist of normal micro-flora and innate immune cells. Most epithelial surfaces have nonpathogenic commensal bacteria micro-flora which secretes some kind of antimicrobial molecules and compete with pathogenic microorganisms for nutrients. When the pathogens overcome these barriers, they are encountered by innate immune cells like macrophages, neutrophils, monocytes, mast cells and dendritic cells. During infection, these immune cells are recruited to the site of infection and rapid response against pathogens, such as engulfing and destroying them, are given.

1.2. Pattern Recognition Receptors

How are pathogens recognized by immune cells? The cells of innate immunity have pattern recognition receptors (PRRs) to recognize pathogens in case of infection. PRRs sense microbes via recognizing pathogen-associated molecular patterns (PAMPs). PAMPs are small molecular motifs conserved within a class of pathogens and they are

vital to microbes for their survival, so that: they do not change these molecules. Some examples of PAMPs are lipopolysaccaride (LPS), peptidoglycan, flagellin and nucleic acids like dsRNA, ssRNA or unmethylated DNA. In addition, PRRs are also able to detect endogenous molecules called danger associated molecular patterns (DAMPs) released by damaged or infected cells. Upon recognition of PAMPs or DAMPs by PRRs, intracellular signaling pathways lead to expression of inflammatory proteins to deal with the infection (Thompson *et al*., 2011).

1.2.1. Toll-Like Receptors

Toll like receptors were the firstly identified pattern recognition receptors and received their names from Toll protein found in *Drosophila melanogaster*. There are thirteen TLRs in mammals. TLRs are type I transmembrane-spanning proteins with extracellular domains with leucine rich repeat (LRR) motifs and an intracellular signaling domain (TIR) homologous to the cytoplasmic domain of IL-1 receptor family members. Upon recognition of Toll specific pathogen associated molecular patterns by the extracellular domain of the TLRs, the signal is transmitted inside the cell through TIR domain-adaptor proteins such as such as MyD88, TIRAP, TRIF and TRAM interactions and the expression of several genes required for inflammatory response is induced (Takeuchi & Akira, 2010).

Each TLR recognizes its subgroup of specific pathogenic components. For example, TLR4 senses lipopolysaccaride (LPS), while unmethylated DNA is recognized by TLR9 which is located in the endosomal compartments of B lymphocytes, monocytes, NK cells and dendritic cells (Latz *et al*., 2004). TLR2 recognizes microbial lipopeptides, whereas TLR5 is essential for sensing of flagellin, and ds-RNA is recognized by TLR3 (Moresco *et al*., 2011).

1.2.2. Nod Like Receptors

The Nod like receptor protein (NLRs) family is one subgroup of the wide repertoire of pattern recognition receptors of the innate immune system. Amoung PRRs, NLRs are cytoplasmic receptors that operate through inflammasomes to induce inflammation and regulate autophagy and cell death pathways. For example, NLRP3 and NLRC4 form inflammasomes upon stimulation with their specific ligands including MSU, ATP, nigericin, etc. Also, other members of the NLR family, NOD1 and NOD2 regulate the NF-κB pathway. In recent years, NLRs started to be considered as key regulators of reproduction, early implantation at fetal-mother interface and embryogenesis, as maternal effect genes which are highly expressed in oocytes and pre-implanting embryos.

NLRs have three functional domains, which are N-terminus protein-protein interaction domain, central oligomerization domain and C-terminus leucine rich repeats (LRRs). The role of the N-terminal domain is signal transduction and activation of inflammatory responses. There are four different classes of the N-terminal protein-protein interaction domain; PYRIN, CARD (Caspase recruitment domain), BIR (Baculoviral inhibitory repeat like domain) and AD (Acidic transactivation domain). The central domain of NLRs, NACHT or NBD, is required for oligomerization of the sensing receptor. For example, NOD1 and NOD2 oligomerize through their central NOD domain to recruit RIP2 kinase via CARD-CARD homotypic interaction upon activation. It is believed that the C-terminal LRR domain is vital for ligand recognition (Barbe *et al*., 2014).

NOD1 and NOD2 are well-known members of the NLR family and they recognize different peptides (iE-DAP and MDP) of bacterial cell wall component peptidoglycan which is a also TLR2 ligand. Upon ligand recognition NOD1 and NOD2 self-oligomerize and they eventually activate the NF-κB transcription factor or MAPK through action of various adaptor proteins including RICK, TAK1 and NEMO

(Hasegawa *et al*., 2008). Finally, activation of these pathways leads to transcription of several inflammatory cytokines and chemokines.

Also, mutations in certain members of the NLR family were associated with various diseases. To illustrate, NLRP2 germline mutations were detected in Beckwith-Wiedeman, which is a fetal overgrowth and familial imprinting disorder (Meyer *et al*., 2009). Also, NLRP7 mutations are linked to the formation of hydatidiform moles which is abnormal human pregnancy, resulting in miscarriage (Radian *et al*., 2013).

1.3. Inflammasomes

The inflammasome is a multi-protein scaffold/complex and consists of caspase-1, ASC, a NLR protein and sometimes caspase-5 molecules with unknown stochiometry. These protein structures are formed in myeloid cells of the innate immune system and they promote activation of zymogens pro-caspase-1 and pro-caspase-5 and maturation of pro-inflammatory cytokines like IL-β and IL-18. Depending on the activator, components of the inflammasomes can vary.

The most well-known example of inflammasomes is the NLRP3 inflammasome. For NLRP3 inflammasome formation, priming and activation signals are required. The initial priming step is the induction of expression of NLRP3, whereas the activation signal is vital for NLRP3 oligomerization and inflammasome assembly. The priming signal is based on signaling cascade through TLR or cytokine receptors. NLRP3 protein levels are tightly regulated via post-translation modifications like ubiquitination in resting conditions, and early priming of NLRP3 is achieved by deubiquitination of NLRP3 through TLR-IRAK1 signaling(Lin *et al*., 2014). In later stages, NLRP3 expression is upregulated by NF-κB, which is a major downstream transcription factor of the TLR or cytokine pathways. Following the priming signal, large repertoire of unrelated ligands (endogenous and exogenous) activate NLRP3 inflammasome formation between NLRP3, ASC and pro-caspase-1 and pro-caspase-1 is converted into active caspase-1 through proximity induced auto-cleavage (Lamkanfi & Dixit, 2014). Some examples of

these unrelated ligands are monosodium urate crystals, elevated ATP levels, asbestos, silica crystals. Then, active caspase-1 processes pro-inflammatory cytokines such as pro-IL-1β and pro-IL-18 into their active forms. The secretion of IL-1β and IL-18 triggers the recruitment of macrophages, monocytes and lymphocytes to the infection site, where edema forms. Pathogens are destroyed by macrophages, dendritic cells and neutrophils and these antigen presenting cells travels to lymph nodes to present pathogenic antigens to T and B lymphocytes for stimulation of the acquired immunity. IL-18 acts by binding to its receptor and induces cell-mediated immunity. Upon activation of NK cells and T cells with IL-18, these cells produce IFN-γ to activate macrophages and other cells (Schroder & Tschopp, 2010). Some members of the NLR family regulate inflammatory responses in a negative way. For example, it was shown that NLRC3 inhibited TLR-dependant activation of NF-κB by interacting with TRAF6 (Schneider *et al*., 2012). Similarly, NLRP10 suppresses auto-processing of Caspase-1 and ASC aggregation (Imamura *et al*., 2010).

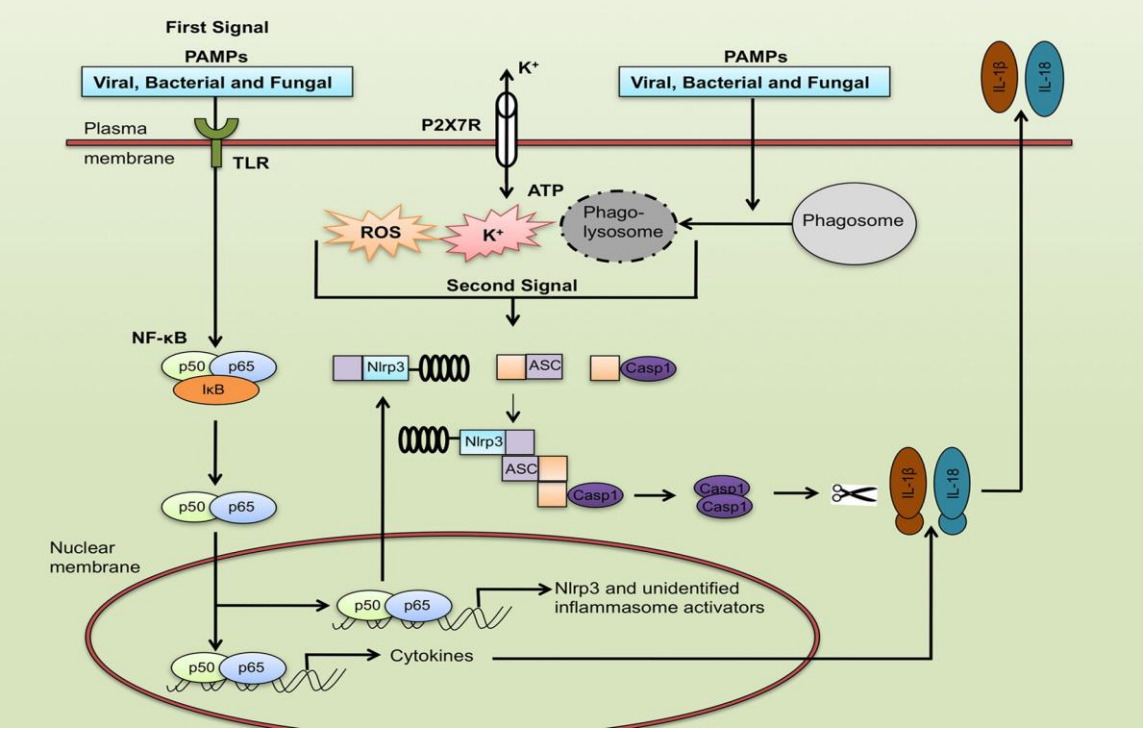

Figure 1.1. NLRs and NLRP3 inflammasome activation (Adopted from Anand *et al*., 2011).

In recent years, NLRP3 was also associated with the newly discovered programmed death events called pyroptosis. Pyroptosis is a Caspase-1 dependent inflammatory cell death. In this process, infected cells produce cytokines, swell, burst and die to attract other immune cells to the inflammation site (Fink & Cookson, 2005). In contrast to apoptosis, pyroptosis occurs within minutes after inflammasome activation, membrane of the pyroptotic cell permeabilizes immediately and cytoplasmic contents are released (Bergsbaken *et al*., 2009). Also, recent papers claim that there is a crosstalk between apoptosis and pyroptosis depending on the strength of the signal. It was shown that AIM2 and NLRP3 inflammasomes activate Caspase-8 to induce apoptotic and pyroptotic cell death. At lower foreign DNA concentrations inside the cell, apoptotic death is promoted whereas pyroptosis occurs rapidly at high DNA concentration (Sagulenko *et al*., 2013). In addition, it was shown that Caspase-8 promotes pyroptosis in wild type DCs while it mediates IL-1β production and apoptosis in Caspase-1 deficient DCs (Antonopoulos *et al*., 2015). Also, Caspase 8 activates NF-κB pathway independent of its pro-apoptotic acticity(Chaudhary *et al*., 2000).

1.4. NLRP13

The NLRP13 gene is located on human chromosome 19 and it has eleven exons. NLRP13 protein has three functional domains; N-terminal PYRIN domain, central oligomerization domain NACHT and C-terminal LRR domain contains seven LRRs.

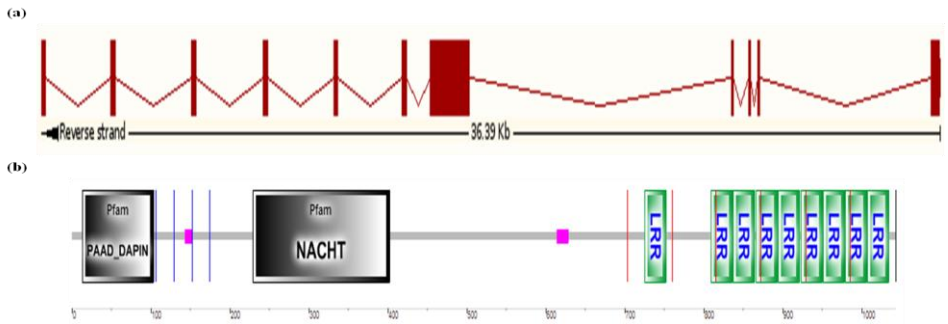

Figure 1.2. NLRP13 schematic structure. (a) NLRP13 gene structure (b) NLRP13 protein domain structure

Our former lab member Yetiş Gültekin, M. Sc. who worked on NLRP13 project previously showed that NLRP13 is mainly localized in the cytoplasm and partially in mitochondria (% 35) using confocal microscopy. It was shown that NLRP13 weakly interacts with inflammatory proteins ASC and Caspase-1 but not with Caspase-5 in co-immunoprecipitation trials. Also, there was an inflammasome-like structure between ASC-Caspase-1 and NLRP13 in overexpression conditions under the confocal microscopy (Gültekin, 2011).

ASC is the adaptor protein of the inflammasomes and it is found to diffuse within the cell in resting conditions. But, it forms ring-like speck structures as inflammasome platforms in infected cells. It was shown that NLRP3 induces ASC speck formations when NLRP3 was transfected with ASC in time and dose dependent manner. Gültekin also showed that there is no significant effect of NLRP13 in ASC speck formation when NLRP13 was transfected with ASC, in time and dose dependent manner in HEK293FT cells (Gültekin, 2011).

Interestingly, NLRP13 is absent in mouse and rat and it is a primate specific gene. NLRP13 has highest homology to NLRP5, which is expressed in mice and has a role in early embryogenesis. Oocytes lacking NLRP5 have abnormal mitochondrial localization and mitochondrial depletion. The absence of NLRP5 leads to the mitochondrial damage, triggering premature activation of mitochondrial pool in oocytes. (Fernandes *et al*., 2012). Also, it was shown that NLRP13 expression is high in oocytes and gradually decreases in developing embryos with a very low expression level in day 5 embryos (Zhang *et al*., 2008). Like NLRP13, other members of the NLR family; NLRP5, NLRP8 and NLRP9, has similar expression pattern. So, these NLR proteins may have regulatory functions in reproduction and early embryonic development.

1.5. Inflammation and Pregnancy

The role of the immune system at the implantation site during pregnancy is more complicated than common knowledge, such that suggested weakness of immune system

creates a risk of infections during pregnancy due to tolerance mechanisms toward fetal tissues. Different from tolerance mechanisms of mother-fetus interactions, NK cells, dendritic cells and macrophages have crucial roles for fetal development during the first trimester of pregnancy, where the lack of these immune cells leads to failures in pregnancy (Mor *et al*., 2011). For proper placentation, trophoblast cells create an inflammatory environment on the epithelium of the uterus by secreting cytokines and chemokines for recruitment and differentiation of immune cells during early phase of fetus-uterus implantation. It was suggested that trophoblasts induce THP1 monocyte cells to secrete inflammatory cytokines such as IL-6, IL-8, MCP-1 and GRO-α at placental-maternal interface. The second stage of pregnancy is the anti-inflammatory phase, when the placenta and growing embryo are not rejected by the mother, while fetus development continues. After completed development of the fetus, another inflammatory phase is again set to deliver the embryo out of mother's womb (Ramhorst *et al*., 2012).

1.6. Immune Privilege

Specific sites of the body have immune privileged status which means the inflammatory immune response is suppressed even if foreign antigens are encountered in these sites. In immune privilege sites, tissue grafts are able to survive for longer time without rejection (Barker & Billingham, 1977). This privileged status is achieved via several strategies: 1) local immunosuppression by certain cytokines and cell surface proteins; 2) MHC class switch, low expression of classical MHC class Ia molecules and high expression of immunoregulatory nonclassical, low polymorphic class Ib MHC molecules in these sites; 3) accumulation of Treg cells around privileged sites creates immune suppressive environment (Streilein, 2003); 4) lack of lymphatic drainage and antigen sequestration behind certain barriers such as blood-brain barrier, blood-testis barrier, etc; 5) Expression of FasL and TRAIL by certain cells are used to kill attacking NK and cytotoxic T cells (Griffith *et al*., 1995). Immune privilege is an evolutionary adaptation to protect vital tissues from the harsh immune responses for proper functioning of these tissues. Without immune privilege at the maternal-fetus interface, where maternal immune cells encounter semiallogeneic fetus, survival of the species would be impossible due to abortions. Some examples of immune privilege areas are brain, hair fol-

licles, testes, the pregnant uterus, the anterior chamber of the eye and the cornea (Niederkorn, 2006).

On the other hand, regulation of immune response is vital for the benefit of the body, so that immune effector cells should be suppressed in the absence of inflammation, later state of the inflammation to protect tissues from potentially damaging effects of an inflammatory immune response. In addition, the immune system is educated to tolerate self-antigens and commensal microorganisms in primary lymphoid organs and peripheral tissues (Barker & Billingham, 1977; Mellor & Munn, 2004).

1.6.1. MHC Expression

Major histocompatibility complex (MHC) molecules are expressed in almost every cell types to present antigens to the immune cells such as T cells and B cells for initiation of pathogen specific adaptive immune responses against foreign molecules. There are two subgroups of MHC molecules; one is MHC Class I molecules that are expressed by all nucleated cells and other is MHC Class II molecules that are specific to APCs (B cells, dendritic cells and macrophages). In immune privilege areas, there is MHC shift in classes of MHC molecules used for antigen presentation, towards immunoregulatory types. For instance HLA-E and HLA-G instead of classical types of HLAs are expressed in immune privileged tissues (Fiszer *et al*., 1997; Ryan *et al*., 2002). Also, there is a decrease in expression levels in MHC molecules to obstruct the presentation of the antigens.

1.6.2. Fas and Trail Ligand Expression

Fas is a TNF family member death receptor that triggers extrinsic apoptotic pathway upon ligand (FasL) binding. FasL expressing cells lead to death of the cell expressing Fas receptor upon Fas-FasL binding and this mechanism is used by the cytotoxic T cells and NK cells for killing their target cell (Huang *et al*., 1999). TRAIL is TNF-

related apoptosis-inducing ligand and it has similar effects on TRAIL receptor expressing cells upon ligand-receptor binding (Wang & El-Deiry, 2003). Also, these mechanisms are one of the strategies of immunosupression in immune privileged sites to remove the antigen specific T cells and prevent antigen specific adaptive immune response activation. For example, interactions between TRAIL and its receptor kill activated lymphocytes to protect placenta against immune cell attach for the proper pregnancy.

2. PURPOSE

NLRP13 is a novel PYRIN domain containing NLR family member and any biological function of NLRP13 is still unknown. NLRP13 RNA expression is very high in oocytes and decreases sharply at blastocyst stage. It was shown that NLRP13 weakly interacts with inflammatory proteins ASC and Caspase-1 and there was an inflammasome-like structure between ASC-Caspase-1 and NLRP13 when overexpressed. It is clear that NLRP13 may have a role in inflammasome regulation in terms of regulation of upstream components of or processing of downstream products like cytokines and chemokines. In this thesis, we further characterized NLRP13 by trying to figure out its roles in inflammasome activity and immune regulation mechanisms. To find which PAMP or DAMP are related with NLRP13, inflammatory molecule treatments were used and the effect of NLRP13 on cytokine processing and secretions were analyzed by WB, ELISA and Cytokine Array. Secondly, it was aimed to produce polyclonal and monoclonal NLRP13 antibodies and study its functions under endogenous experiment conditions and to identify its interaction partners, to find how it regulates inflammatory pathways and to produce NLRP13 knock-down and overexpression lines THP1 monocytes and cells derived immune privileged tissues were generated for functional experiments. High NLRP13 expression in oocytes can be a clue for the importance of NLRP13 early implantation during pregnancy. For this purpose, the effect of NLRP13 on inflammation during the implantation and immune tolerance mechanisms during later stages of pregnancy were investigated by using knockdown and overexpression cell lines in co-culture experiments.

3. MATERIALS

3.1. Cell Lines

3.1.1. Human Embryonic Kidney Cell Line (HEK293FT)

The HEK293FT cell line was kindly provided by Prof. Maria Soengas from the Spanish National Cancer Research Center (CNIO, Madrid, Spain) and grown in DMEM supplemented with 10% FBS, 2mM L-Glutamine, 1x MEM Non-Essential Aminoacids, 100 U/ml penicillin and 100 µg/ml streptomycin.

3.1.2. THP1 Monocytic Cell Line

The THP1 cell line was kindly provided by Prof. Ahmet Gül from the Istanbul University, (Istanbul, Turkey) and grown in RPMI supplemented with 10% FBS, 2mM L-Glutamine, 1x MEM Non-Essential Aminoacids, 100 U/ml penicillin and 100 µg/ml streptomycin.

3.1.3. Swan71 Throphoblast Cell Line

The Swan71 cell line was purchased from the American Type Culture Collection, Virginia, USA and grown in DMEM supplemented with 10% FBS, 2mM L-Glutamine, 1x MEM Non-Essential Aminoacids, 100 U/ml penicillin and 100 µg/ml streptomycin.

3.1.4. F0 Myeloma Cell Line

F0 myeloma cell line (CRL-1646) was kindly provided by Fatıma Yücel Ph. D. from TUBİTAK Marmara Research Center, (Gebze, Turkey) and grown in DMEM supplemented with 20% FBS, 2mM L-Glutamine, 1x MEM Non-Essential Aminoacids, 100 U/ml penicillin and 100 µg/ml streptomycin.

3.2. Chemicals, Plastic and Glassware

All chemicals used in this study were purchased from either Sigma (USA), Applichem (Germany) or Merck (Germany). Plastics from TPP (Switzerland), tips and tubes from Axygen (USA) were used throughout the study. Glassware, tips and tubes were sterilized by autoclaving at 121°C for 20 minutes before use.

3.3. Buffers and Solutions

3.3.1. Cell Culture

Table 3.1. Cell culture materials.

DMSO	AppliChem, Germany
0.5 % Trypsin-EDTA 1X	Gibco Invitrogen, USA
Dulbecco's Modified Eagled Medium (DMEM)	Gibco Invitrogen, USA
RPMI Media 1640	Gibco Invitrogen, USA
McCoy's 5A (modified) Medium	Gibco Invitrogen, USA
Fetal Bovine Serum	Gibco Invitrogen, USA
MEM Non-essential amino acid (NEAA) 100X	Gibco Invitrogen, USA

Table 3.1. Cell culture materials (cont.).

Penicillin/Streptomycin	Gibco Invitrogen, USA
PBS 10X	80 gr NaCl 2 gr KCl 2.4 gr KH_2P0_4 14.4 gr Na_2HPO_4 Add ddH_2O up to 1 lt (pH 7.2)
PMA	Sigma, USA
LPS	Sigma, USA
Puromycine	Sigma, USA
R837	Sigma, USA
Alum	Sigma, USA
ATP	Sigma, USA
MSU	Sigma, USA

3.3.2. Cloning and Analytic Digestion

Table 3.2. Enzymes used in cloning experiments.

Restriction Enzymes	NEB, England
T4 DNA Ligase	NEB, England

3.3.3. Agarose Gel Electrophoresis

Table 3.3. Buffers and solutions used for agarose gel electrophoresis.

DNA Ladder	DNA Ladder Mix Fermentas, Canada

Table 3.3. Buffers and solutions used for agarose gel electrophoresis (cont.).

50X Tris Acetic acid EDTA (TAE)	2 M Tris-acetate 50 mM EDTA pH 8.5
Loading Dye	6x Loading Dye Fermentas, Canada
Ethidium Bromide (EtBr)	Merck

3.3.4. Culture of Bacteria

Table 3.4. Solutions for liquid and solid bacterial culture.

LB Agar	1 L LB medium 15 g Agar
LB Medium	10 g Tryptone 5 g Yeast Extract 5 g NaCl
Ampicillin (1000X = 100 mg/ml in 70% EtOH)	AppliChem, Germany
Kanamycin (1000X = 50 mg/ml in ddH_2O)	Sigma-Aldrich, USA
Chloramphenicol	Sigma-Aldrich, USA
Terrific Broth	12 gr Tryptone 24 gr Yeast Extract 4 ml Glycerol 100 ml 10X Potassium PO_4 Buffer
1 M KPO_4 Buffer	Add 1 M KH_2PO_4 onto 1 M K_2HPO_4 until pH 7.2

3.3.5. Protein Purification

Table 3.5. Solutions for protein purification.

1 M IPTG	Roche, Germany
Dough's Solution	167 mM Tris-HCl (pH 6.8) 0.5 % SDS 10 % Sucrose 25 µl/ml B-mercaptoethanol 0.01 % Bromophenol Blue
Elution Buffer	50 mM Tris-HCl 150 mM NaCl 0.1 mM EDTA pH 7.5
Coomassie Solution	0.1 % Coomassie Brilliant Blue R-250 10 % Acetic Acid 50 % Methanol
Destaining Solution	10 % Acetic Acid 50 % Methanol
PBS 10X	80 gr NaCl 2 gr KCl 2.4 gr KH_2P0_4 14.4 gr Na_2HPO_4 Add ddH_2O up to 1 lt (pH 7.2)

3.3.6. Antibody Production

Table 3.6. Solutions for antibody production.

F5881 Freud Adjuvant Complete	Sigma-Aldrich, USA

Table 3.6. Solutions for antibody production (cont.).

F5506 Freud Adjuvant Incomplete	Sigma-Aldrich, USA
PEG	Merck, USA
HAT 50X	Gibco Invitrogen, USA
Sodium Citrate Glucose	2.3 gr Sodium Citrate 0.8 gr Citric Acid 2.2 gr D-Glucose Add ddH_2O up to 100 ml

3.3.7. Transfection

Table 3.7. Solutions for transfection.

2X HBS Buffer	50 mM HEPES pH 7.0 280 mM NaCl 1.5 mM Na_2HPO_4
$CaCl_2$	Merck, USA
HEPES	Gibco Invitrogen, USA
HP Xtreme Gene Transfection Reagent	Roche, Germany

3.3.8. Protein Isolation

Table 3.8. Solutions for protein isolation.

Protease Inhbitor Cocktail	Roche, Germany
Cell Lysis Buffer	0.2 % NP-40, 142 mM KCl, 5 mM $MgCl_2$, 10 mM Hepes, 1 mM EDTA

3.3.9. Western Blotting.

Table 3.9. Chemicals for Western Blotting.

Acrylamide: Bisacrylamide	30 gr Acrylamide 0.8 gr Bisacrylamide in 100 ml ddH_2O
Ammonium Persulfate	10 % APS (w/v)
Blocking Solution	5 % BSA in TBST
Lumi-Light Western Blotting Solution	Roche, Germany
SuperSignal West Femto Maximum Sensitivity Substrate	Pierce, USA
Bovine Serum Albumin Fraction V	Roche, Germany
Protein Ladder (PI-26617)	Pierce, USA
15 % Resolving Gel	500 ml Acrylamide: Bisacrylamide 10 ml 10 % SDS 200 ml 1.875 M Tris pH 8.8 Add ddH_2O up to 1 lt
10 % Resolving Gel	333 ml Acrylamide: Bisacrylamide 10 ml 10 % SDS 200 ml 1.875 M Tris pH 8.8 Add ddH_2O up to 1 lt
4 % Stacking Gel	3.3 ml Acrylamide: Bisacrylamide 6.3 ml 0.5 M Tris-HCl pH 6.8 250 µl 10 % SDS Add ddH_2O up to 25 ml
Running Buffer	1X Tris-Glycine Buffer 0.1 % SDS
6X Laemmli Sample Buffer	1.2 gr SDS 6 mg Bromophenol Blue 4.7 ml Glycerol 1.2 ml 0.5 M Tris pH 6.8 500 µl B-mercaptoethanol Add ddH_2O up to 10 ml

Table 3.9. Chemicals for Western Blotting (cont.).

SDS	AppliChem, Germany
10X TBS	90 gr NaCl 121.14 gr Tris-Base pH 7.5 Add ddH_2O up to 1 lt
TBS-Tween	1X TBS 0.1 % Tween 20
TWEEN	CalbioChem, Canada
Transfer Buffer	39 mM Glycine 48 mM Tris-Base 0.0625 % SDS
10X Tris-Glycine Buffer	15 gr Tris-Base 72 gr Glycine Add ddH_2O up to 500 ml
2-Propanol	Merck, USA
TEMED	Merck, USA
PVDF membrane	Roche, Germany
Methanol	Merck, USA
Sodium Azide	Roche, Germany

3.3.10. ELISA

Table 3.10. Solutions for ELISA.

Wash Buffer	0.05 % Tween 20 in 1X PBS
Reagent Diluent	1% BSA in 1X PBS
Subsrate Solution	1:1 mixture of Color Reagent A (H_2O_2) and Color Reagent B (Tetrametylbenzidine)
Stop Solution	2 N H_2SO_4

3.3.11. Immunoprecipitation

Table 3.11. Chemicals for Immunoprecipitation.

Pierce Protein A/G Agarose, 15 ml resin	Pierce, USA
IP lysis buffer	0.5 % NP-40, 500 mM Tris-HCl, pH 8, 137 mM NaCl, 2 EDTA

3.4. Fine Chemicals

3.4.1. Plasmids

Table 3.12. Plasmids used in this study.

pENTR 1A no ccdb	Tamer Önder Lab (KU, Sarıyer, Turkey)
pcDNA3-HA-NLRP13	AKIL (Apoptosis and Cancer Immuno. Lab)
pcDNA3-Flag-NLRP13	AKIL (Apoptosis and Cancer Immuno. Lab)
pcDNA3-Myc-NLRP13	AKIL (Apoptosis and Cancer Immuno. Lab)
pcDNA3-GFP-NLRP13	AKIL (Apoptosis and Cancer Immuno. Lab)
pet30a-NLRP13	AKIL (Apoptosis and Cancer Immuno. Lab)
pcDNA3-Flag-Caspase5	Nunez Lab, University of Michigan
pcDNA3-procaspase-8	Nunez Lab, University of Michigan
pcDNA3-procaspase-8 MT	Nunez Lab, University of Michigan
pcDNA3-procaspase-9	Nunez Lab, University of Michigan
pcDNA3-procaspase-9 MT	Nunez Lab, University of Michigan
pcDNA3-procaspase-12	Nunez Lab, University of Michigan
pcDNA3-caspase 11	Nunez Lab, University of Michigan
pcDNA3-procaspase-1	Nunez Lab, University of Michigan
plex307 lentiviral	NCTE Lab, Bogazici University

3.4.2. Primers

Table 3.13. Sequences of primers used in this study.

Primer Name	**Aim**	**Sequence**	**Tm (C^o)**	**RE Cutting Site**
NLRP13-PYD-F	Cloning	AGTTGCGGCCGCAATGAACTTTTCTGTAATC	61.7	Not I
NLRP13-LRR-R	Cloning	TTATGATATCTCATTACCCGAGTTTCTGCAGCCT	62	EcoRV
pENTR-F	Sequencing	CTACAAACTCTTCCTGTTAGTTAG	50.3	-
NLRP13_Seq_F1	Sequencing	AGAAGCAGCAGCAGGGAATA	58.8	-
NLRP13_Seq_F2	Sequencing	GGTTCCCCTGGCTACCTTAC	58.3	-
NLRP13_Seq_F3	Sequencing	CATTCCACAAAGCCACAAGA	58.1	-
NLRP13_Seq_F4	Sequencing	ACGTGCAAATCGGTAACTCC	58.5	-
NLRP13_reverse seq	Sequencing	AGTAGGCGCTGCAGTTCCTC	59.5	-

3.4.3. Antibodies

Table 3.14. Antibodies used in this study.

Antibody	Host/Isotype	Company	Concentration	Purpose
B-actin	Rabbit	Cell Signaling	1:1000	WB
FLAG	Rabbit	Cell Signaling	1:1000	WB
ASC	Mouse	Matsumoto	1:1000	
Rabbit IgG	HRP	Cell Signaling	1:2000	WB
Mouse IgG	HRP	Cell Signaling	1:2000	WB
NLRP13 (2C11)	Mouse	Homemade	1 µg/ml	WB
NLRP13 (19D5)	Mouse	Homemade	1 µg/ml	WB
NLRP13 (41C)	Mouse	Homemade		WB
IL-1β	Mouse	Cell Signaling	1:1000	WB
IgG from murine serum	Mouse	Roche, Germany	-	IP
Polyclonal NLRP13	Rabbit	Santa Cruz	1:2500	WB

3.5. Kits

Table 3.15. Kits used in this study.

High Pure PCR Purification Kit	Roche, Germany
High Pure RNA Isolation Kit	Roche, Germany
High Pure Plasmid Isolation Kit	Roche, Germany
Genopure Plasmid Midi Kit	Roche, Germany
ImPromII-Reverse Transcription System	Promega, USA
Antibody Spin Trap	GE Healthcare

3.6. Equipment

Table 3.16. Equipment used in this study.

Autoclaves	MAC 601, Eyela, Japan ASB260T, Astell, UK
Centrifuges	Allegra X22-R, Beckman, USA Himac CT4200C, Hitachi Koki, Japan J2-MC Centrifuge, Beckman, USA J2-21 Centrifuge, Beckman, USA
Freezers	2021D, Arçelik, Turkey 4250T, Arçelik, Turkey
Incubator	Hepa ClassII Forma Series, Thermo, USA
Heat Block	VWR, USA
Laminar Flow Cabinets	Class II A, Tezsan, Turkey Class II B, Tezsan, Turkey
Magnetic Stirrer	Yellowline MSH Basic, USA
Microscopes	Zeiss, Axio Observer, Germany Z1 Inverted Mic., Germany Leica, TCSSP5II, Germany Nikon, Eclipse TS100, Japan
Microwave Oven	Arçelik,Turkey
pH Meter	H221, Hanna Instr., USA
Pipettes	Gilson, USA
Plate reader	VersaMax, Molecular Devices, USA
Sonicator	SonoPlus, Bandelin, Germany
Spectrofluorometer	Cary Eclipse, Agilent Tehnologies, USA
Pipettors	Greiner-bio one, UK RatioLab acupetta, Germany
Power Supplies	EC135-90, Thermo lectron Corp Power Pac Universal, BIO-RAD, USA
Western Blot Visualization	Stella, Raytest, Germany
Scales	Precisa XT4200C, Germany

Table 3.16. Equipment used in this study (cont.).

SDS-PAGE Electrophoresis System	Mini-PROTEAN 4Cell, BIO-RAD, USA
SDS-PAGE Transfer System	Trans-Blot Semi-Dry, USA
Shakers	Polymax 1040, USA Polymax 1010, USA Heildophl, Germany
Spectrophotometer	Nanodrop ND-100 Thermo, USA
Vortex	Fisons Whirli Mixer, UK GmcLab, Gilson, USA
Water Bath	GFL, Germany Memmert, Germnay
Water filter	UTES, Turkey

4. METHODS

4.1. Cell Culture

4.1.1. Maintenance of Cell Lines

The HEK293FT, Swan71 and Hec1A cells were washed with 1X PBS and trypsin was used for subculturing. The immortal F_0 Myeloma cells were subcultured by scraping gently and THP1 cells are non-adherent acute monocytic leukemia cells. Freezing medium of each cell line was their special media with 10 % DMSO and 15 % FBS.

4.2. Generation of Stably NLRP13-expressing Cell Lines

4.2.1. Cloning into pENTR 1A no ccdb Vector

pENTR 1A (no ccdb) vector was kindly provided by Assoc. Prof. Tamer Önder from Koc University (Istanbul, Turkey). Not I and EcoR V restriction enzymes in multiple cloning site of the vector were selected for cloning. Open reading frame of NLRP13 (NM_176810.2) was found from NCBI database. NotI restriction enzyme cutting site was included at the 5' end of the NLRP13 forward primer and EcoRV restriction enzyme cutting site was added to the 5' end of the NLRP13 reverse primer. NLRP13 was amplified with Q5 DNA Polymerase using the designed primers, and the expected PCR products were loaded in 1% agarose gel and they were extracted and purified with a PCR purification kit. 2 μg purified PCR products and pENTR 1A vector were digested with Not I and EcoR V restriction enzymes in double digestion reaction and digestion products were purified again with PCR purification kit (Roche, Germany).

For the ligation reaction, digested vector and PCR products were ligated using T4 DNA ligase (NEB, USA). In this reaction, 30 ng digested plasmid was used and the reaction was done at 4°C with 1:5 (vector: insert) ratio overnight. Ligation products were transformed into Stable3 competent *E. coli* bacteria. Positive colonies were detected with pENTR F and Reverse Seq 2 primers in colony PCR. For further verification of plasmids, they were sent to Macrogen (Macrogen, Netherlands) for sequencing.

4.2.2. Cloning into plex 307 Lentiviral Vector via Gateway Cloning System

In the Gateway® cloning system, recombination process between donor vector and destination vector occurs and the gene of interest is inserted between the special sites of the donor vector is transferred into destination vector after the recombination. For the NLRP13 cloning, pENTR 1A NLRP13 is the donor vector and pLex 307 was the lentiviral destination plasmid. LR reaction was done at 25°C overnight using 75 ng donor vector, 75 ng destination vector, 1 µl LR Clonase and 1 µl TE buffer. On the next day, 0.5 µl Proteinase K solution was added to LR mixture to stop the reaction and the mixture was transformed into DH5α competent *E. coli* bacteria. Positive colonies were selected with NLRP13 forward and reverse primers in colony PCR. For further verification of plasmids, they were sent to Macrogen (Macrogen, Netherlands) for sequencing.

4.3. Transfection

4.3.1. Calcium Phosphate Transfection of HEK293FT Cells

HEK293FT cells are easily transfected by calcium phosphate transfection method which produces insoluble precipitates of plasmid DNA and calcium phosphate that are engulfed by the HEK293FT cells. 10^6 HEK293FT cells were seeded into 6 well plates 16 hours before transfection and incubated overnight at 37°C and 5 % CO_2 incubator. Plasmid mixture was prepared according to experiment and mixed with ddH_20, 2 M $CaCl_2$

and 2X HBS solution with mixing by tapping tube in the given order, with the amounts indicated in Table 4.1. After 5 minutes incubation, the mixture was added dropwise onto the cells. On the next day, transfection efficiency was checked by fluorecsent protein expression under fluorescent microscope.

Table 4.1. Recipie of Transfection Mixture.

Plate Type	**DNA**	**dd$H_2$0 (add up to)**	**2M $CaCl_2$**	**2X HBS**
6-well plate	0.5-1 µg	219.5 µl	30.5 µl	250 µl

4.3.2. Transfection via X-tremeGENE HP DNA Transfection Reagent

Swan71, THP1, HEC1a and Tera-2 cells are not transfected easily via calcium phosphate transfection, so that; X-tremeGENE HP DNA Transfection Reagent was used for these cell lines. Cells were seeded 16 hours before transfection and incubated over-night at 37°C and 5 % CO_2 incubator. Total DNA was diluted with appropriate serum-free medium to a final concentration of 0.01 µg/µl and mixed gently. Final amount of X-tremeGENE HP DNA Transfection Reagent using 1:3 ratio was pipetted directly into medium containing DNA and the transfection reagent: DNA complex was incubated for 20 minutes at RT. After 20 minutes incubation, the mixture was added dropwise onto the cells. 8 hour later, fresh medium was given to the cells. On the next day, the transfection efficiency was checked by fluorecsent protein expression under fluorescent microscope.

Table 4.2. Recipie of Transfection Mixture.

Plate	**Transfection mixture volume per well(µl)**	**DNA(µg)**	**Final amount of reagent(µl) using 1:3 ratio**	**Cell Density**
12 well plate	100	1	3	$25x10^4$
6 well plate	200	2	6	$5x10^5$

4.3.3. Lentiviral Transduction

For stable overexpression or knockdown experiments, lentiviral transduction can be used, where viral particles are produced when pCMVdeltaR8.74 and pDM2.G lentiviral packaging plasmids together with desired construct of interest in special lentiviral plasmid are co-transfected in HEK293 FT cells. 1 µg lentiviral vector, 750 ng pCMVdeltaR8.74 and 250 ng pDM2.G plasmids were co-transfected in 6.10^6HEK293 FT cells in 6 well plate and virus containing media were collected into eppendorf tubes with polybrene 2 days after transfection. These viruses then were used to infect target cell types. Target cells were seeded at 1.10^6 cells per well of 6 well plates and 500 µl viruses were given to each well for 12 h and then virus containing media were removed. Depending on the application, antibiotic selection was done until killing of all infection negative cells. In our case, 1 µg/ml puromycine was used to select positive cells.

4.4. Generation of Antibodies against NLRP13

4.4.1. IPTG Induction and Nickel Chromatography

pET30-NLRP13 vector (cloned by Yetiş Gültekin) was transformed into Rosetta DE3 pLysS *E. coli* bacteria, inoculated into 5 ml Terrific Broth containing kanamycin and chloramphenicol and incubated at 37^{o}C for overnight. On the next day, 5 ml bacteri-

al culture was added into 250 ml Terrific Broth containing kanamycin and chloramphenicol and shaked at 37^{o}C. When OD_{600} was between 0.6-1, 250 µl 1 M IPTG was given to bacterial culture and shaked overnight at 23^{o}C. After induction, purification of His-tagged NLR13 protein was attempted using His Bind Quick Purification Cartridges (Novagen, USA) but all trials were unsuccessfull.

4.4.2. NLRP13 Protein Purification from Gel Slices

Purification of NLRP13 using His Bind Quick Purification Cartridges was not achieved, possibly due to high molecular weight of NLRP13 (118 kDa) and NLRP13 making insoluble precipitates as an inclusion body. Bacterial culture was centrifuged at 7500 g for 10 minutes and the bacterial pellet was suspended with 1X PBS containing 1% Triton X-100. The bacterial suspension was sonicated 10 times, 3 seconds 3x50% power program in ice and centrifuged at 4500 g for 5 minutes. Sonication and centrifugation steps were repeated two more times and the bacterial pellet was collected each time. Triton X-100 makes proteins precipitate more as inclusion body and preliminary purification was achieved and the pellet was finally dissolved into 1X PBS. Dough's Solution was added to the final bacterial suspension and boiled at 90 °C for ten minutes. Then, the protein solution was loaded into 10% polyacrylamide gel with two wells (one small well for ladder and other large well for protein lysate). After electrophoresis for a certain time, the gel was cut from above 100 kDa and below 130 kDa, excised gel was crushed well with elution buffer (50 mM Tris-HCl, 150 mM NaCl, 0.1 mM EDTA pH 7.5) and homogenized gel-buffer solution was shaked at 30°C overnight. On the next day, the solution was centrifuged at 10000g for 10 minutes and the supernatant containing proteins was collected at -20°C. Protein concentration was quantified by comparing with BSA standards via SDS-PAGE.

4.4.3. Immunization

His-tagged NLRP13 purified from gel slices was injected to 5 Balb/c mice and one rabbit for immunization every 15 days during a 45 day procedure. 50 µg NLRP13

was injected with Freud Adjuvant Complete for the first injection and Freud Adjuvant Incomplete for further injections. The injection volume was 400 µl (200 µl+200 µl adjuvant) for rabbit injections and 200 µl (100 µl+100 µl adjuvant) for mice injections. After the injection procedure, blood was taken into tubes containing sodium citrate glucose from animals and blood serum containing our antibodies was obtained by centrifugation at 13000 rpm for 15 minutes. Finally, blood serum was tested via ELISA and Western Blotting and anti-NLRP13 polyclonal serum aliquots were stored at -20^{o}C for further studies.

4.4.4. Monoclonal Antibody production via Hybridoma Technology

Monoclonal NLRP13 antibodies were produced via classical Hybridoma Technology which allows fusion of antibody-producing mouse B cells from Balb/c mice with immortal human myelomas in tissue culture conditions. Before fusion procedure, 6000 feeder cells (primary mouse peritoneal macrophages) per well were seeded into 96 well plate. These feeder cells were isolated from different Balb/c mouse by injecting 5 ml DMEM with intraperitoneal injection and taking DMEM back containing blood cells. Then, the cell suspension was centrifuged at 2000 g for 2 minutes, the bigger white cells (peritoneal macrophages) were counted and seeded.

On the next day, our immunized mice were sacrificed and their spleens were isolated for fusion procedure. Single spleen cell suspension was obtained by dissociating isolated spleen mechanically in 1X PBS. Spleen cells were washed two times with 1X PBS by centrifugation at 900 rpm for 10 minutes. In parallel, F_0 myelomas were washed two times. Both cells were counted and they were mixed with 1:5 F_0 myeloma: Spleen cell ratio and centrifuged at 2000 g for 2 minutes. Then, cell pellet was dissolved with 1 ml pre-warmed PEG slowly in 60 seconds and waited for 60 seconds at 37°C. Then, 4 ml DMEM without FBS and antibiotics was added to the suspension slowly in 2-3 minutes and then 20 ml DMEM without FBS and antibiotics was added slowly in 2-3 minutes. Finally, 20 ml DMEM with 20% FBS was added to the suspension slowly in 2-3 minutes and waited the mixture at 37°C for 1 hour. After one hour incubation, cells

were centrifuged at 2000 g for 2 minutes, suspended with 50 ml DMEM (10% FBS and 1X HAT) and 100 µl cell suspension per well was seeded into 96 well plate containing feeder cell.

Ten days after the fusion step, colonies were selected by visual inspection and screened using ELISA. The most promising clones were also controlled via Western Blooting and positive clones were grown in bigger plates. The next step was isolation of single hybridoma cell, for this purpose clones were seperated to single cell, in a one cell per well form, to obtain pure monoclonal antibody producing colonies. Colonies, derived from single cell, were screened with ELISA and Western Blotting again and three different candidate clones producing monoclonal anti-NLRP13 antibody were stocked at -80^{o}C. For purification of NLRP13 antibodies, the positive clones were grown in DMEM without FBS and Antibody Spin Trap was used to purify NLRP13 monoclonal antibodies.

4.5. Treatments

1x10^{6} THP1 cells per well were differentiated with 0.5 µM PMA in 6 well plates for 3 hours. Then, PMA-containing RPMI medium was removed and fresh media were given to the cells. On the next day, the cells were treated with different chemicals as seen as in Table 4.3.

Table 4.3. Concentration and duration of the treatment.

Chemicals	**Concentration**	**Time**
LPS	500 ng/ml	3 hours
MSU crystals	25 µg/ml-50 µg/ml	3 hours after LPS
Alum	0.5 mg/ml-1 mg/ml	3 hours after LPS
ATP	2 mM-4 mM	30 minutes after LPS
R837	2,5 µg/ml-5 µg/ml	3 hours after LPS

Table 4.3. Concentration and duration of the treatment (cont.).

Doxorubicin	0,5 µg/ml	24 hours
Etoposide	0,5 µg/ml	24 hours
Tamoxifen	25 nM	6 hours

4.6. Western Blotting

4.6.1. Preparation of Samples

Cell culture samples were collected with a scraper, centrifuged at 2000 g for 2 minutes, washed with 250 µl 1X PBS and harvested with 100 µl cell lysis buffer (for 6 well plate) by incubating on ice for 1 hour while vortexing periodically. After 1 hour lysis step, the cells were centrifuged at 13000 rpm for 30 minutes at 4°C. Following centrifugation step, supernatant was collected and mixed with 20 µl 6X Laemmli sample buffer. Finally, samples were ready to load into SDS-PAGE gels after boiling at 95°C for 10 minutes.

4.6.2. Preparation of SDS-PAGE Gels

Mixture of 8 ml of resolving gel with 80 µl 10% APS and 8 µl TEMED was poured between casting glasses and the gel was covered with 2-propanol for flat gel surface. After resolving gel polymerization, 2-propanol was removed. Mixture of 3 ml of stacking gel with 30 µl 10% APS and 3 µl TEMED was poured onto polymerized resolving gel and the comb was inserted. After stacking gel polymerization, the gel was put into a vertical electrophoresis tank and the tank was filled with 1X running buffer.

4.6.3. Protein Gel Electrophoresis and Semi-dry Transfer

The denatured samples were loaded and SDS-PAGE was run at 80 V until samples entered resolving gel and the voltage was arranged to 120 V until samples reached to the end of resolving gel. During proteins run, filter papers and PVDF membrane were cut according to the size of the gel. The filter papers were wetted in cold transfer buffer while PVDF membrane was activated in methanol. Activated PVDF membrane was also put in the transfer buffer after washing in ddH_2O and 2 filter papers were placed on transfer apparatus. Then, the membrane, the gel and two more filter papers were placed on the filter papers like gel-membrane sandwich. Finally, transfer was performed at 10 V for 45 minutes.

4.6.4. Membrane Blocking, Antibody Incubation and Visualization

The PVDF membrane was taken into a plastic box and blocked with 5% BSA in TBS-T solution for 1 hour at RT by shaking. The membrane was incubated with primary antibody solutions at 4°C overnight. Antibody solution was prepared by dissolving primary antibody at a 1:1000 ratio in 5% BSA with sodium azide. On the next day, unbound and non-specific antibodies were removed by washing the membrane three times with TBS-T for 5 minutes and the membrane was incubated with 1:2000 secondary antibody solution at RT for 1 hour. Secondary antibody was conjugated to HRP enzyme and was chosen according to the animal where the primary antibody was produced. After three washes with TBS-T for 5 minutes, solutions of Lumi-Light Western Blotting Solution (Roche, Germany) were mixed with 1:1 ratio and this mixture was added onto the membrane. Visualization of the membrane was done by using a digital visualization device (Stella, Raytest, Germany). When the membrane was used for different protein detection, it was washed with TBS-T and new primary antibody solution was given to the same membrane without stripping it.

4.7. ELISA

4.7.1. Plate Preparation

100 µl of the diluted Capture antibody was coated into 96-well ELISA plate and incubated overnight at room temperature after sealing the plate well. On the next day, the samples were washed with ELISA wash buffer three times. Then, the plate was blocked with 200 µl Reagent Diluent and incubated at room temperature for a minimum of one hour. Before assay procedure, washing steps were repeated.

4.7.2. ELISA Assay Procedure

100 µl of standard or sample was added in Reagent Diluent per well and incubated for two hours at room temperature. After washing steps, 100 µl of diluted Detection antibody was added to each well and incubated for two hours at room temperature. Then, 100 µl of working dilution of Streptavidin-HRP was given per well for 20 minutes at room temperature after washing steps. After streptavidin addition, samples should be kept at dark as possible. Then, 100 µl of Substrate solution was added to each well for 20 minutes at RT after washing the samples with Was buffer. Finally, 50 µl of Stop solution was added to samples and optical density of the samples was detected by subtracting the readings at 530 nm from readings at 450 nm.

4.8. ASC Speck Purification

THP1 cells stably expressing ASC-GFP and NLRP13 were treated with 250 ng/ml LPS and 5 mM ATP for ASC speck formation. Then, the cells were collected with centrifugation at 2000 rpm for 2 min. The cell pellet of 150 cm plate was dissolved in 3 ml 1X cold PBS and sonicated three times 5 seconds 3x 10%, 50% power program on ice. Then, the cell lysate was centrifuged at 2400 g for 5 minutes and vortexed suddenly

until see clear DNA fragments. The lysate containing fragments was left for gravity sedimentation for 10 minutes and supernatant was collected into a new falcon for centrifugation at 200 g for 5 minutes. Then, the supernatant was discarded and the pellet was dissolved in 10 ml 1X cold PBS by vortexing. The gravity sedimentation step was repeated and the supernatant was centrifuged at 200 g for 60 minutes. Finally, the pellet was dissolved in 10 ml 1X cold PBS, the solution was passed through 5 µm filter. At the filter step, ASC specks remains in the filter. To get the specks, 1X cold PBS was reapplied to the filter in the opposite direction until clear PBS flow. PBS containing specks was centrifuged at 2400 g for 60 minutes and the pellet was dissolved in 50 µl 1X cold PBS.

4.9. Immunoprecipitation

50 µl of Protein A/G bead per well was washed with lysis buffer three times by centrifugating at 13.000 rpm for 30 seconds. Then, 250 µl 1X PBS containing corresponding antibody was given to the washed beads and rotated on orbital shaker for 60 min at RT. At the same time, 15.10^6 cells were lysed with 500 µl lysis buffer on ice for 20 min, centrifuged at 13.000 rpm for 30 min at 4°C and supernatant was kept as protein lysate. After antibody-bead conjugation, they were washed to remove unbounded antibodies with lysis buffer three times by centrifugating at 13.000 rpm for 30 seconds. Then, protein lysate was given to the antibody bounded-beads and rotated on orbital shaker overnight at 4°C after 50 µl protein lysate was kept as whole cell lysate (WCL). On the next day, samples were washed with lysis buffer three times by centrifugating at 13.000 rpm for 30 seconds. Then, samples were solved in 50 µl Laemmli sample buffer and stored at -20°C for further analysis.

4.10. Cytokine Array

To see effect of NLRP13 on cytokine secretions, we purchased Human Inflammation Antibody Array (Roche, Germany) which contains forty inflammatory cytokines. In this array, specific cytokine antibodies were conjugated to specific dots of array

membrane and cocktail of biotin conjugated anti-cytokines are used to find specific cytokines on their dots. THP1-NLRP13 and THP1 control cells were differentiated with 10 μM PMA for 3 hours and then cells were incubated 48 hours in cell culture conditions. After 48 hours, the cell supernatant of THP1-NLRP13 and THP1 empty cells was collected and used in Inflammation Antibody Array. Firstly, array membranes were incubated with 1X Array blocking buffer for 30 min at RT and put 1 ml of serum for each sample on the membrane and incubate overnight at 4°C. On the next day, the membranes were washed with 1X Array wash buffer 1 for 5 min three times and with 1X Array wash buffer 2 for 5 min three times. Then, 1 ml of 1X Biotin-Conjugated Anti-Cytokines was given to each membrane and incubated for 2 hours at RT. The membranes were washed as previous washes and 2 ml of 1X HRP-Conjugated Streptavidin was given for 2h incubation at RT. After washes as before, (1:1) mixture of Detection Buffer C and Detection Buffer D was put on the membranes and cytokines were detected by chemiluminescence via CCD cameras of Stella imaging system.

For analysis of the array data, positive control spots were used to normalize spot densities. Positive control spots are provided with biotin-conjugated IgG and there are 6 positive spots on each membrane. Each cytokine's signal was normalized by dividing them to average of positive signals as measured by STELLA. Then, fold change in cytokine secretions was calculated by dividing normalized cytokine signals of THP1 NLRP13 sample to THP1 empty ones.

4.11. THP1 Education by Swan71 Throphoblasts' Conditioned Medium

As mentioned before, trophoblast cells create an inflammatory environment on epithelium of the uterus by secreting cytokines and chemokines for recruitment and differentiation of immune cells during early phase of fetus-uterus implantation. To see effect of NLRP13 on these events, Swan71 cells stably expressing NLRP13 was used. 12.10^5 Swan71-control, Swan71-NLRP13 and Swan71- NLRP7 cells were seeded in T-25 flasks with 2% FBS medium and incubated for 2 days in cell culture conditions. Then, 1 ml of Swan71 conditioned medium was given to 1.10^6 THP1 cells to educate

them for 6, 12, 24 and 48 hours. After specific time points, cells were lysed for Western Blotting and sera were collected for ELISA. Hec1A cells were used as a negative control because they do not secrete molecules for education of THP1 macrophages.

5. RESULTS

5.1. Bioinformatic Analysis of NLRP13 Expression

NCBI GEO Datasets store gene expression Datasets, as well as original Series and Platform records in the Gene Expression Omnibus (GEO) repository. Analysis using data from this repository shows that NLRP13 expression is very high in oocytes and early stages of embryonic development (Figure 5.1).

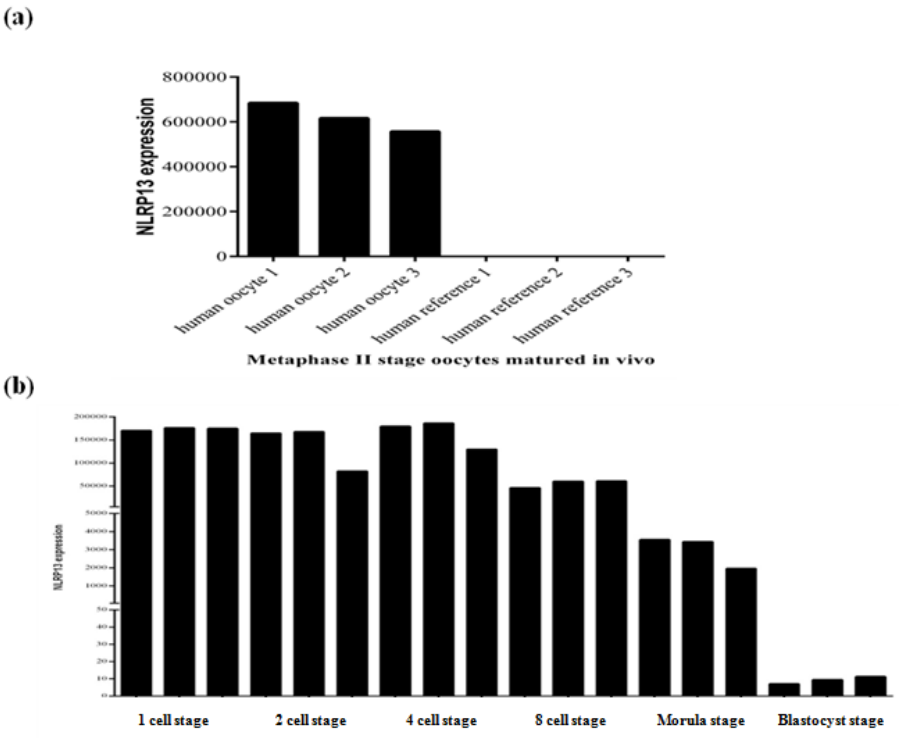

Figure 5.1. NLRP13 expression is high in oocytes and embryos until blastocyst stage.

When NLRP13 expression was investigated from databases, it is again seen that there is high NLRP13 expression in oocytes. Additionally, CD4 T-large granular lymphocytes express NLRP13 at medium level (Figure 5.2.). Furthermore, there is high NLRP13 expression in ovaries and placenta according to Human Protein Atlas.

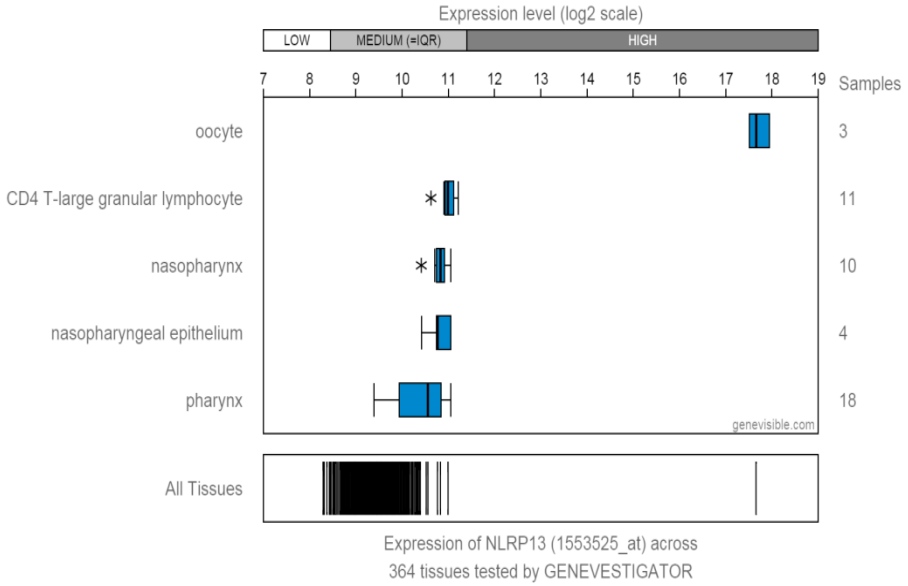

Figure 5.2. NLRP13 is highly expressed in oocytes. NLRP13 expression was investigated across 364 tissues by GENEVESTIGATOR and top five tissues were shown in log2 scale.

5.2. Endogenous Protein Expression of NLRP13 in Human Cell Lines

Due to the lack of commercially available NLRP13 antibodies, we aimed to produce polyclonal and monoclonal NLRP13 antibodies for our planned functional experiments. For this purpose, pet30a-His NLRP13 cloned by Yetiş Gültekin M. Sc., was used. His-NLRP13 protein was purified. IPTG induced NLRP13 expression and purified NLRP13 was detected via Commassie staining (Figure 5.3a and b). Rabbit serum was collected as anti-NLRP13 polyclonal antibody after 4 rounds of immunization. Sera were tested by Western Blotting analysis on protein extracts taken from HEK293-FT cells overexpressing different constructs of NLRP13 and it is seen that NLRP13 serum recognizes GFP-NLRP13, Flag-NLRP13 and HA-NLRP13 in HEK 293 FT cells. GFP-NLRP13 is calculated to be around 136 kDa while Flag-NLRP13 and HA-NLRP13 are 119 kDa. The polyclonal anti-NLRP13 serum was able to detect the three NLRP13 constructs at their expected sizes, whereas there were some additional nonspecific bands also observable (Figure 5.3).

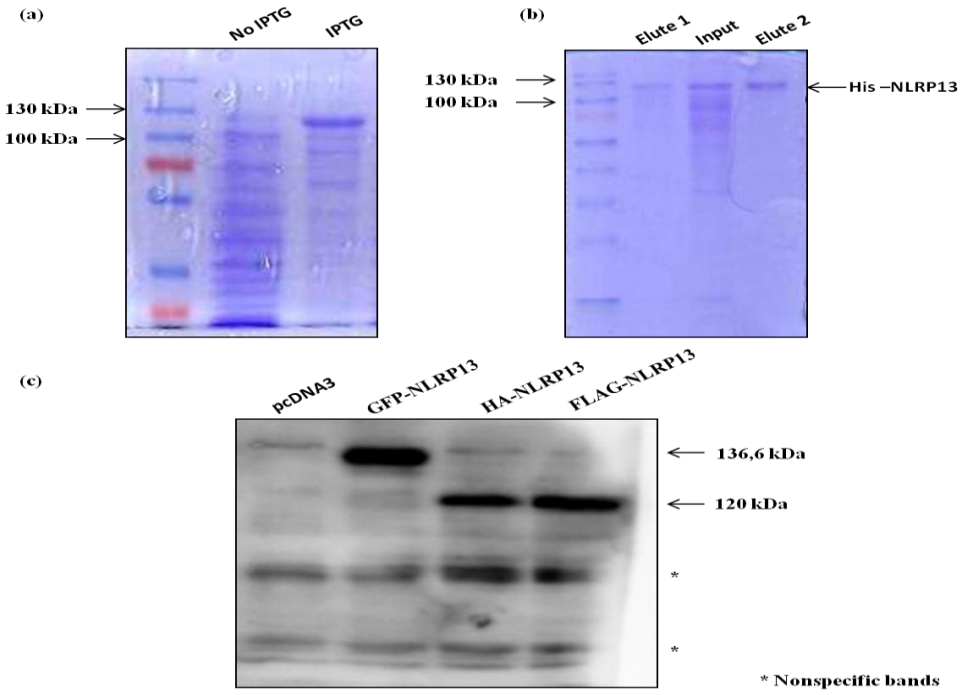

Figure 5.3. Purification of NLRP13 and Production of anti-NLRP13 serum in rabbits. (a) NLRP13 was expressed upon IPTG induction in Rosetta strains. (b) Successful purification of His-NLRP13 was detected via Commassie staining. (c) 1:200 rabbit serum recognizes different NLRP13 constructs via WB.

In order to generate monoclonal anti-NLRP13 antibodies, classical hybridoma technology was used. To do this, Balb/c mice were used for 4 rounds of immunization. Post-immunization collected serum samples were analyzed by ELISA and Western Blotting as previously described. To do this, blood sera were taken and used in WB and ELISA to test whether the sera contained antibodies against His-NLRP13. No bands were expected for sera of negative control 1X PBS. After making sure that both mice were immunized nicely with His-NLRP13, their spleens were extracted and used for fusion with F_0 Myeloma cells. Positive clones were selected via ELISA. However, only a few positive clones worked well in Western Blotting. To test specificity of the clones, NLPRP3, NLRC3, NLRP7 and NLRP13 proteins were over-expressed in HEK293FT cells and protein extracts were tested using sera obtained from hybridoma clones 2C11and 19D5.

Both clones were NLRP13 specific and did not recognize the other NLRs (Figure 5.4). In all protein extracts, a non-specific band at 80 kDa was observed.

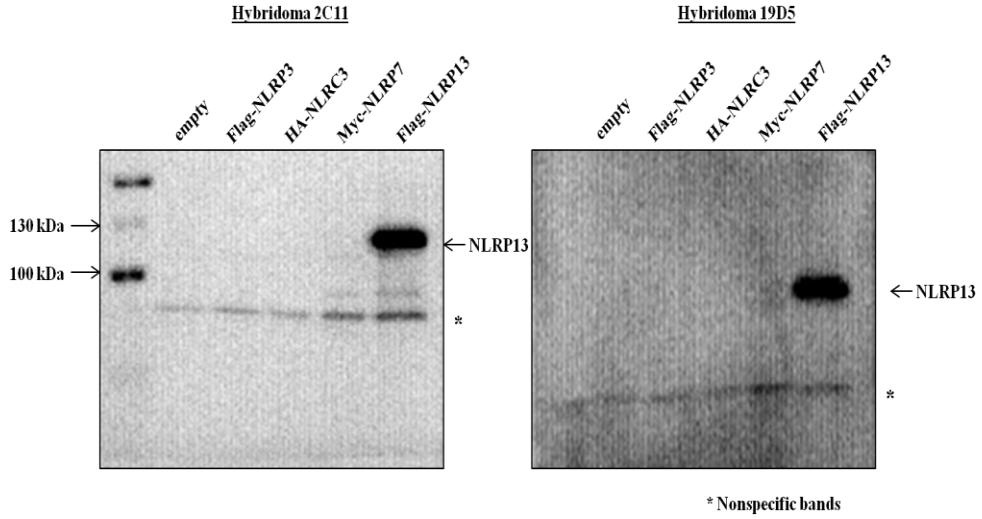

Figure 5.4. Monoclonal NLRP13 antibodies specifically recognize NLRP13. (a) Serum from clone 2C11 was used in WB. (b) Serum from clone 19D5 was used in WB.

5.2.1. Endogenous NLRP13 Protein Expression in Cell Lines

To investigate the biological roles of NLRP13, a major aim was to identify cells that express NLRP13 highly or not expressing at all. High NLRP13 expressing cells can be used for knockdown experiments and stable overexpression of NLRP13 can be possible in low NLRP13 expressing cells. In order to detect NLRP13 expression in our commonly used cell lines, 1.10^6 cells per line were lysed and NLRP13 levels were detected by Western Blotting. For expression analysis, immune cells such as T cells and monocytes and cells derived from immune privileged sites were used. Hec1A and Hec1B are endometrial carcinoma cell lines, whereas Jar and Swan71 are placental carcinoma and throphoblast cell lines. THP1 cells are monocytes and Jurkat cells are T lymphocytes in origin. Raw cells which are mouse macrophage cells were used as a negative control, because NLRP13 is primate specific gene and it is absent in mouse.

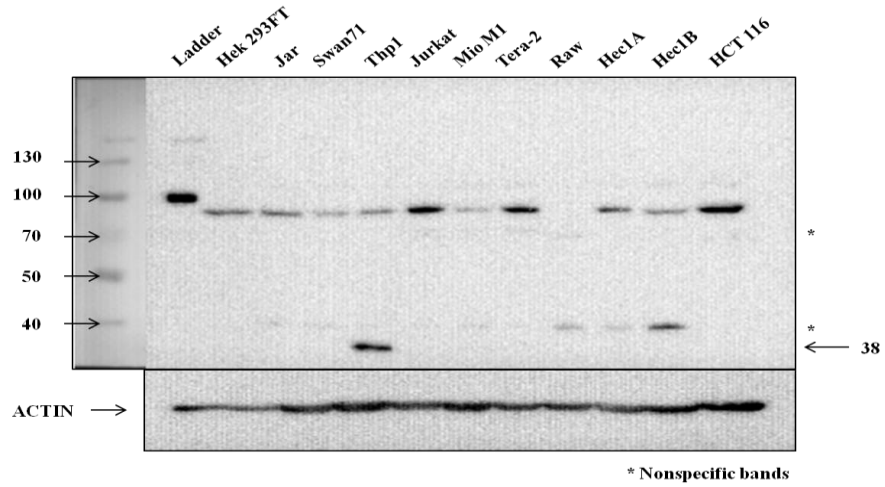

Figure 5.5. Endogenous NLRP13 protein expression in different cell lines.

Normally, the calculated molecular weight of NLRP13 is 119 kDa. However, the monoclonal Ab (2C11) generated in this study detected a nearly 90 kDa protein in all cell lines except Raw macrophages. Additionally, a 38 kDa protein was detected in THP1 monocytes (Figure 5.5).

5.2.2. Proteolytic Processing of NLRP13

During expression analysis of NLRP13, lower unexpected molecular-weight proteins were also detected. Analysis of the primary amino acid sequence of NLRP13 revealed possible caspase cleavage sites (Table 5.1). The PROSPER webserver predicts protease subsrates and their corresponding cleavage sites based on the primary amino acid sequence. This webserver uses three different models and gives possible cleavage sequences and sites for each model.

Table 5.1. Possible Caspase cleavage sites of NLRP13.

Model 1		Model 2		Model 3	
Possible cleavage site	Possible cleavage sequence of amino acid	Possible cleavage site	Possible cleavage sequence of amino acid	Possible cleavage site	Possible cleavage sequence of amino acid
291	DWPD FDAP	175	EEAD HRRK	473	DLAD DSWP
293	PDFD APIE	291	DWPD FDAP	489	LAIE GLWS
328	SLDD GSPC	473	DLAD DSWP	506	TEIE GLEV
470	AEVD LADD	662	FEVD LNIL	966	DLQD DGVK
473	DLAD DSWP	853	LQDD GIKL	1023	LDTD GVKM
732	HLED LSNS	966	DLQD DGVK		
966	DLQD DGVK	967	LQDD GVKL		
1023	LDTD GVKM	1023	LDTD GVKM		

Taking into account these observations, we wondered whether NLRP13 is processed by proteolytic enzymes post-translationally. To answer this question, NLRP13 was co-transfected with different caspases in HEK 293FT cells and NLRP13 was detected by Western Blotting. Firstly, it was observed that NLRP13 levels decreased sharply when it was cotransfected with Caspase 8 or 9 (Figure 5.6a). Then, NLRP13 was cotransfected with Caspase 8, 9 or their mutant versions. As seen in Figure 5.6b, 38 kDa fragment was detected after cleavage of NLRP13 by Caspase 8 or 9 but not when transfected with the mutant forms of Caspase 8 or 9. Increasing concentrations of Caspase 8 or 9 did not have additional affects on the cleavage pattern. We did not observe the 38 kDa fragment when homemade polyclonal NLRP13 Ab was used (Figure 5.6a).

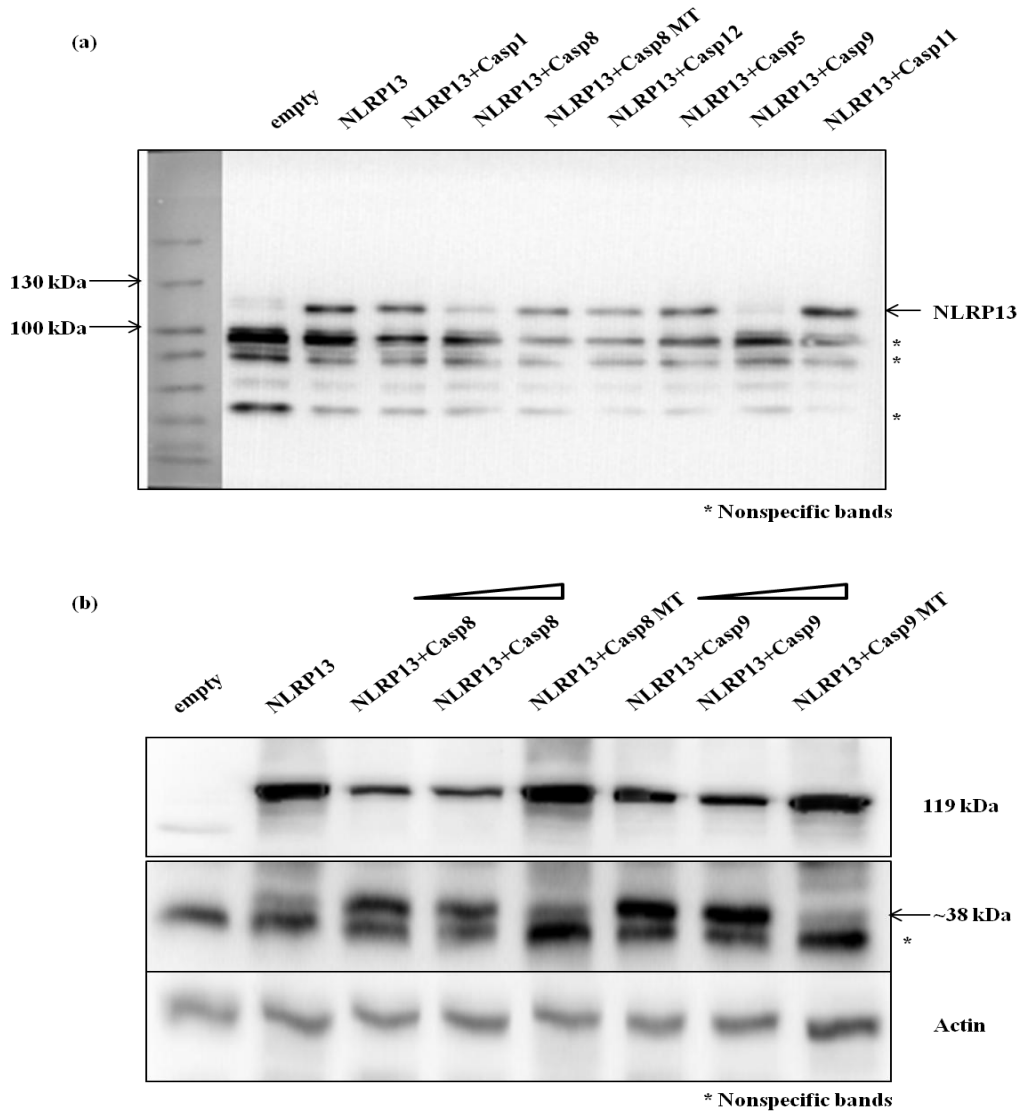

Figure 5.6. Processing of NLRP13 by Caspases 8 and 9. (a) NLRP13 was detected by homemade polyclonal NLRP13 Ab via WB. (b) NLRP13 was detected by commercial polyclonal NLRP13 Ab via WB and Actin was used as a loading control.

For further characterization of NLRP13 processing, we wondered whether NLRP13 is processed by Caspases during apoptosis. To do this, Tera-2 cells which undergo apoptosis upon doxorubicin treatment were used. Doxorubicin is an anti-cancer drug that triggers apoptosis. GFP tagged NLRP13 and empty vector pcDNA3 were transfected in Tera-2 cells and the cells were treated with 1 µg/ml doxorubicin for 12 hours one day after transfection. When GFP-NLRP13 expressing cells were treated with doxorubicin,

GFP-NLRP13 is cleaved and degraded. Interestingly, the 38 kDa fragment is present in untreated GFP-NLRP13 and this fragment was also lost upon doxorubicin treatment (Figure 5.7).

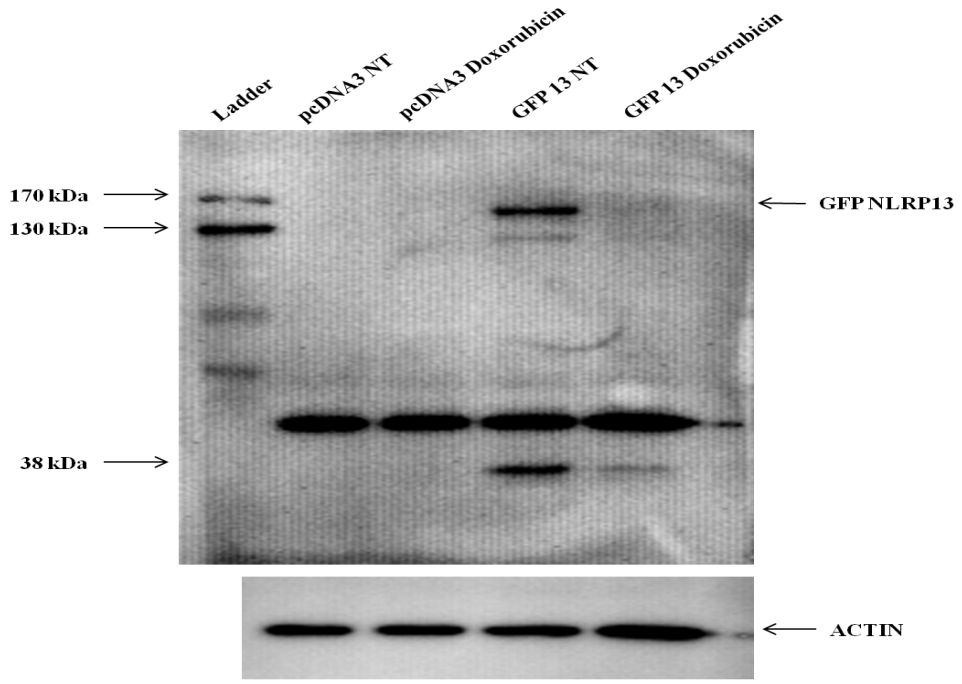

Figure 5.7. Processing of NLRP13 upon doxorubicin treatment in Tera-2 cells. Transfected cells were treated with 1 μg/ml doxorubicin for 12 hours and NLRP13 protein levels were detected with the commercial polyclonal NLRP13 Ab via WB and Actin was used as a loading control.

5.3. Study of Endogenous Interaction Partners of NLRP13

Knowledge about interaction partners of a protein can help to make predictions about the function of a protein. Because NLRP13 is a novel NLR family member, we wanted to figure out interaction partners of NLRP13. For this purpose, NLRP13 was immune-precipitated by using the monoclonal Ab (2C11) and mouse polyclonal Ab in the Swan71 cell line. Then, IP samples were detected by monoclonal Ab (2C11) via Western Blotting. As we can see in Figure 5.8a, it is seen that both monoclonal and polyclonal antibodies immunoprecipitated the same band whose molecular weight is about

90 kDa. This band is absent in the IgG control IP sample. Also, two smaller bands are seen in the monoclonal Ab (2C11) sample. Then, these samples were sent to mass spectrometry analysis to identify interaction partners of NLRP13. IP samples of NLRP13 were detected by SDS-PAGE before mass analysis. Mass analysis was done by nanoLC-MS/MS (Thermo Easy nano LC Q-Exactive). In this analysis, each sample was divided into two samples; one sample is upper part of antibody heavy chain and other one is below part of antibody heavy chain.

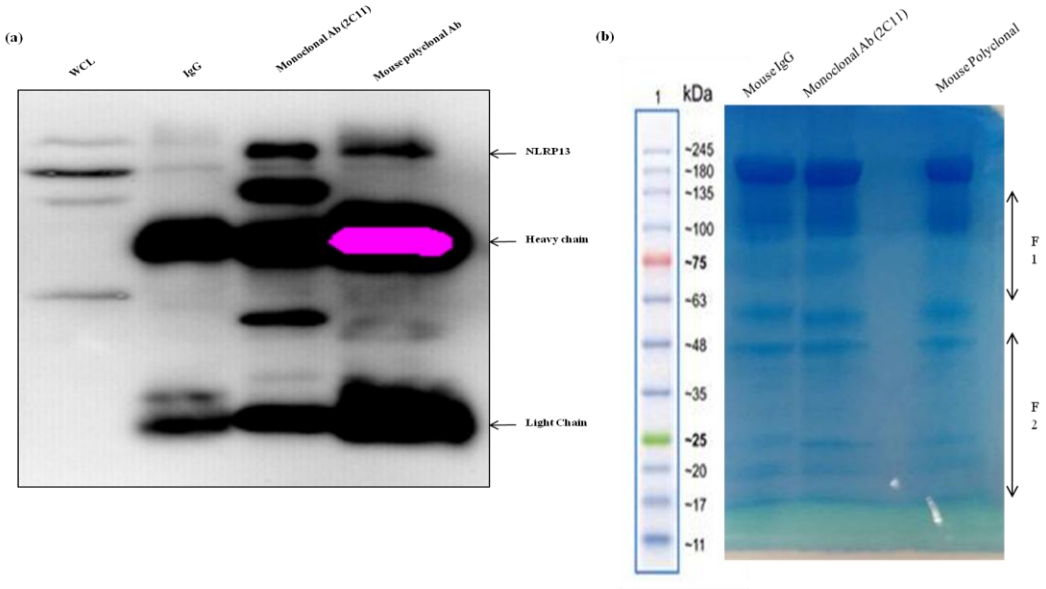

Figure 5.8. Immunoprecipitation of NLRP13 for mass spectrometry analysis. (a) IP samples of NLRP13 were detected by 2C11 NLRP13 monoclonal Ab via WB. (b) IP samples were detected by Commassie staining before mass spectrometry analysis.

Normally, it was expected to get a high amount of peptides from NLRP13 in our experiment groups and other proteins with lower quantity of specific peptides are possible interaction partners if these proteins were absent in precipitates by control IgG. In spectrometry mass analysis, peptides from NLRP13 were detected in only the F1 fraction of polyclonal NLRP13 but amount of NLRP13 was very low to identify interaction partners of NLRP13, for which we detected only three peptides (Table 5.2). For this rea-

son, we were unable to find any interaction partners of NLR13 in this analysis. The low amount of NLRP13 in the IP samples can result from low expression of NLRP13 in cells although NLRP13 could be detected in Western Blotting experiments.

Table 5.2. Mass spectrometry analysis of NLRP13 immunoprecipitations using polyclonal anti-NLRP13.

Description	**Coverage**	**Unique Peptides**	**Peptides**	**PSMs**	**AAs**	**MW(kDa)**
Uncharacterized protein	3,85	1	1	2	208	22,6
Uncharacterized protein	3,85	1	1	2	208	24,1
35 kDa protein	3,82	1	1	1	314	34,6
cDNA FLJ56352, highly similar to Succinyl-CoA ligase subunit alpha	3,63	1	1	1	248	26,5
Four and a half LIM domains protein 3	3,57	1	1	2	280	31,2
Uncharacterized protein	3,43	1	1	1	233	24,7
Otoancorin isoform 3	3,40	1	4	6	1060	117,8
NLRP13	3,36	1	3	3	1043	118,8
Protein	3,35	1	1	1	209	23,7
Uncharacterized protein	3,20	1	1	1	250	27,3
Chondroitin sulfate proteoglycan 4	3,19	1	6	7	2322	250,4

In mass spectrometry analysis, Coverage means that default the percentage of the protein sequence covered by identified peptides. PSMs display the total number of identified peptide sequences (peptide spectrum matches) for the protein, including those redundantly identified. Aas is default the sequence length of the protein. As can be seen in Table 5.2, coverage of NLRP13 is very low (3.36).

Then, NLRP13 was immunoprecipitated in NLRP13 overexpressing THP1 cells for mass spectrometry analysis. To do this, NLRP13 was inserted into the genomic DNA as stably transfected via lentiviral transduction. As can be seen in Figure 5.9a, NLRP13 immunoprecipitation was done very well and these samples were sent for mass spectrometry analysis. Figure 5.9b shows a band around 119 kDa via SDS-PAGE. But, again there were only four NLRP13 peptides in the positive IP samples (Table 5.3 and Table 5.4). Again, we were unable to find any interaction partners of NLR13 in this analysis. As mentioned before, it was expected to get a high amount of peptides from NLRP13 and other proteins with lower quantity of specific peptides are possible interaction partners if these proteins were absent in precipitates by control IgG. Unfortunately, the amount of NLRP13 was very low again to identify interaction partners of NLRP13. These unexpected findings may result from the inability of 2C11 monoclonal NLRP13 antibody to work in immunoprecipitation experiments.

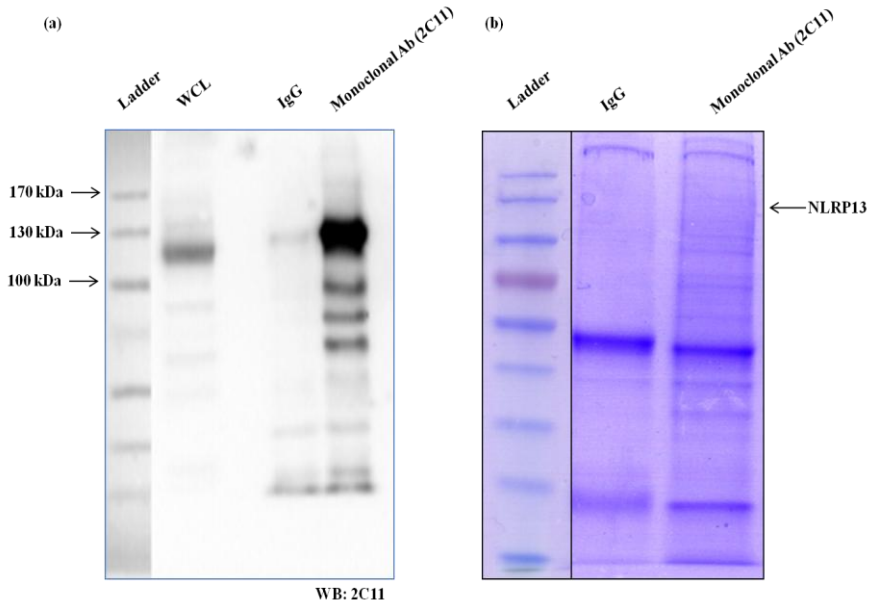

Figure 5.9. NLRP13 immunoprecipitation using 2C11 NLRP13 Ab. (a) NLRP13 was detected by mAb 2C11 via WB. (b) IP samples were detected by Commassie staining before mass spectrometry analysis.

Table 5.3. Unique peptides identified in mass spectrometry analysis of proteins after NLRP13 immunoprecipitation.

Identified Proteins	**Molecular Weight**	**IgG Control**	**Sample**
Lysine-specific demethylase 3B	192 kDa	0	4
Membrane-associated progesterone receptor component 1	22 kDa	2	4
Microtubule-associated protein RP/EB family member 1	30 kDa	0	4
Mitochondrial genome maintenance exonuclease 1	39 kDa	0	4
Moesin	68 kDa	6	4
NACHT, LRR and PYD domains-containing protein 13	119 kDa	0	4
Nascent polypeptide-associated complex subunit alpha, muscle-specific form	205 kDa	2	4
Nuclear fragile X mental retardation-interacting protein 2	76 kDa	5	4
Nuclear pore complex protein Nup205	228 kDa	0	4
Nucleus accumbens-associated protein 1	57 kDa	0	4
Peroxiredoxin-4	31 kDa	2	4
Persulfide dioxygenase ETHE1, mitochondrial	28 kDa	0	4

Table 5.4. Unweighted spectrum of mass spectrometry analysis of proteins after NLRP13 immunoprecipitation.

Identified Proteins	**Molecular Weight**	**IgG Control**	**Sample**
DNA-directed RNA polymerase II subunit RPB1	217 kDa	0	4
Rho-associated protein kinase 2	161 kDa	0	4
Isoform 5 of Glycogen debranching enzyme	173 kDa	0	4
Calcineurin B homologous protein 1	22 kDa	0	4

Table 5.5. Unweighted spectrum of mass spectrometry analysis of proteins after NLRP13 immunoprecipitation (cont.).

Isoform 2 of Structural maintenance of chromosomes flexible hinge domain-containing protein 1	216 kDa	0	4
NACHT, LRR and PYD domains-containing protein 13	119 kDa	0	4
Isoform 2 of DNA (cytosine-5)-methyltransferase 1	185 kDa	0	4
Isoform 2 of NAD kinase 2, mitochondrial	46 kDa	0	4
Heat shock protein beta-1	23 kDa	0	4
Short/branched chain specific acyl-CoA dehydrogenase, mitochondrial	47 kDa	0	4
AP-3 complex subunit sigma-1	22 kDa	0	4
Synaptobrevin homolog YKT6	22 kDa	0	4

5.4. Generation of stably-NLRP13-expressing Cell Lines

In order to be used in functional experiments stably NLRP13 expressing cell lines were produced.

5.4.1. Cloning of NLRP13 into pENTR1A no ccdb Vector

NLRP13 (1043 bp) was amplified with Q5 DNA Polymerase by using designed primers, 2 μg purified PCR products and pENTR 1A vector were digested with NotI and EcoRV enzymes in double digestion reaction and digestion products were purified again with PCR purification kit. Ligation products were transformed into Stable3 competent bacteria. Positive colonies were detected with pENTR F and Reverse Seq 2 primers in colony PCR. Expected PCR product size for positive clones was 450 bp. Colonies 2 and

7 gave us expected PCR product (Figure 5.10). Further verification of plasmids, they were sent to Macrogen for sequencing and colony 7 was found to be mutation free.

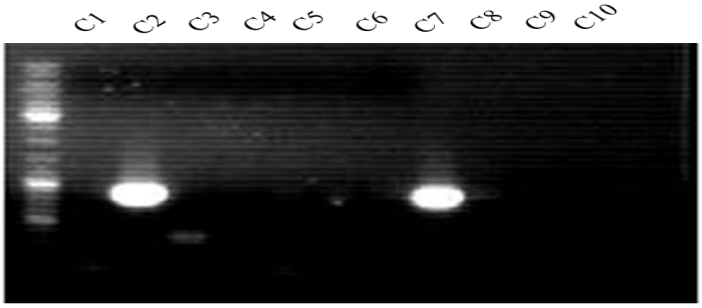

Figure 5.10. Cloning of NLRP13 into pENTR1A donor vector and colony PCR for selection of positive clones.

5.4.2. Cloning of NLRP13 into plex 307 Lentiviral Vector via Gateway® System

After cloning of NLRP13 into pENTR1A vector, NLRP13 was cloned into pLEX 307 lentiviral vector via Gateway® cloning system. In this cloning system, LR reaction mixture was transformed into DH5α competent bacteria. Positive colonies were selected with NLRP13 forward and reverse primers in colony PCR. For further verification of plasmids, they were sent to Macrogen for sequencing and colony 9 was mutation free.

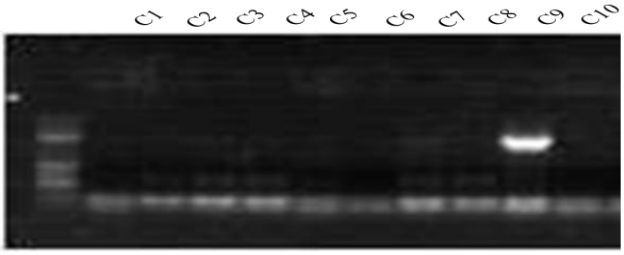

Figure 5.11. Cloning of NLRP13 into pLEX 307 lentiviral vector and colony PCR for selection of positive clones.

After successful cloning of NLRP13 into the lentiviral vector, lentiviral particles were produced and used for transduction and stable expression of NLRP13 in THP1, HEC1A, and Swan71 and Tera-2 cells. Puromycine was used to select the cells expressing NLRP13. Here, it can be seen that NLRP13 overexpression was done well in Tera-2 cells (Figure 5.12).

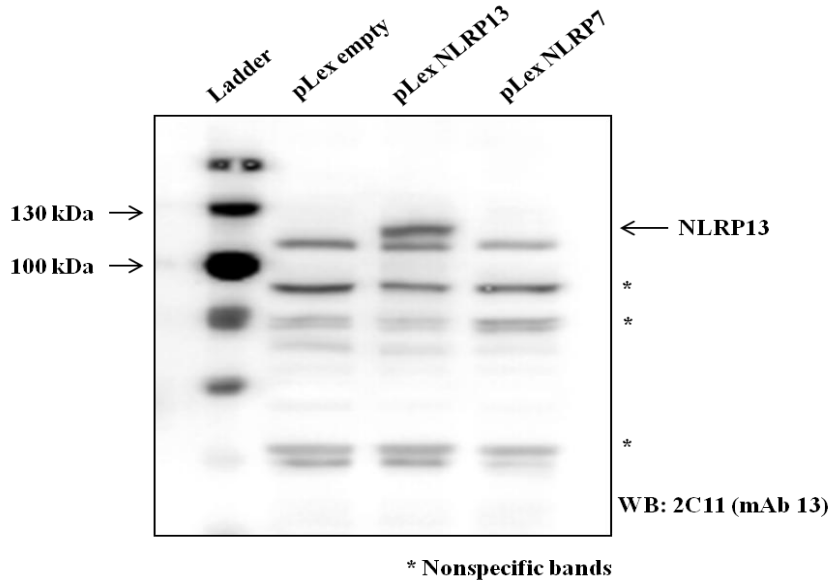

Figure 5.12. Stable NLRP13 expression in Tera-2 cells.

5.5. Study of Putative Upstream Regulators of NLRP13

Nod-like receptors can sense different PAMPs and DAMPs during inflammation. Depending on the inflammatory signal, expression of a certain NLR can change. For example, NLRP3 expression is upregulated by NF-κB after LPS is recognized by TLR4. To find which PAMP or DAMP can change NLRP13 expression, inflammatory chemical treatment was done in THP1 macrophages. Knowing which inflammatory molecules change NLRP13 expression is important to figure out which inflammatory pathways are related with NLRP13. For this purpose, different inflammatory molecules were used to

induce inflammation in THP1 cells and NLRP13 expression levels were analyzed depending on the signal.

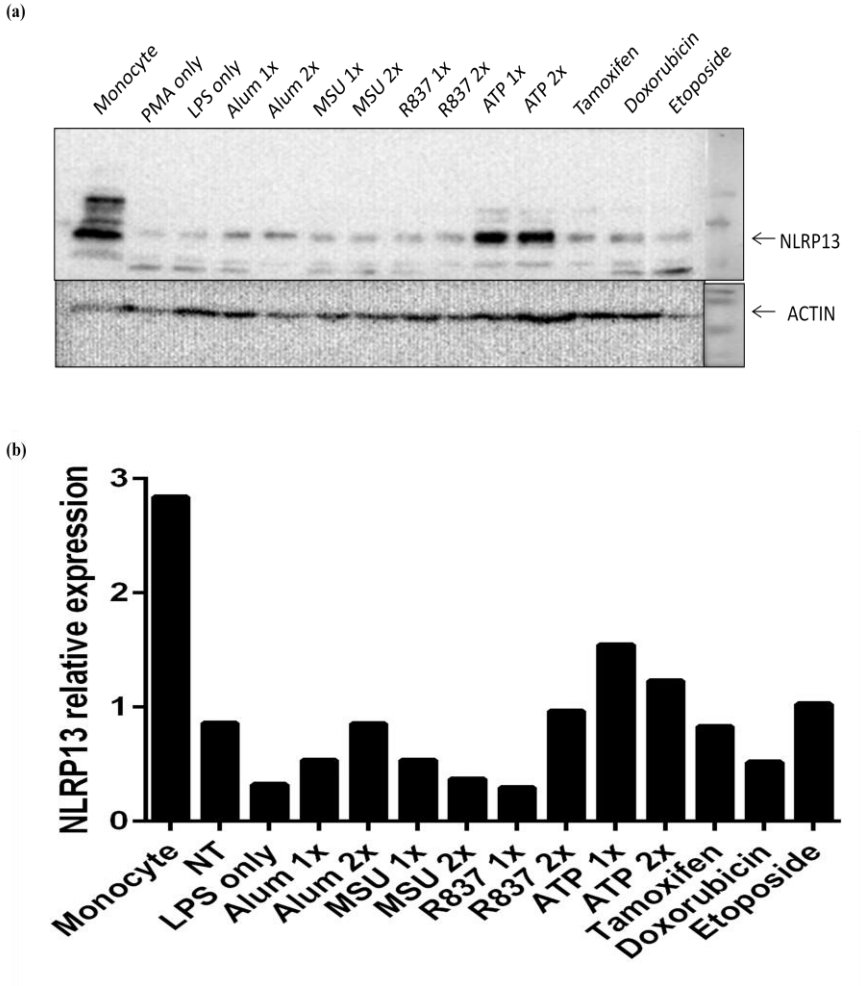

Figure 5.13. Effect of inflammasome activators on NLRP13 protein levels in THP1 cells. (a) NLRP13 levels were detected by WB. (b) NLRP13 was normalized to Actin.

THP1 cells are monocytic cells that require a signal to differentiate into macrophages. Upon a 3 hour PMA treatment, THP1 monocytes differentiate into macrophages and attach to the plate. On the next day, LPS was used as a priming signal for 3 hours and different inflammatory chemicals were used as a second signal for inflammasome activation. After specific treatment time for each molecule, cells were lysed and NLRP13 levels were analyzed via Western Blotting (Figure 5.13a). NLRP13 levels were normalized to Actin (Figure 5.13b). Quantification of NLRP13 levels after Western Blotting shows

that NLRP13 expression decreases after differentiation of monocytes into macrophages (Figure 5.13b). A further decrease in NLRP13 level was observed upon LPS priming. Comparing all tested inflammasome activators here, ATP appears to be the most potent activator of NLRP13 where for both concentrations of ATP NLRP13 expression increased by almost five-fold. Observation of a sharp decrease in NLRP13 expression after differentiation of monocytes into macrophages leaded us to perform another experiment. We wondered whether the decrease in NLRP13 protein level is due to decrease in NLRP13 expression or post-transcriptional events. To understand this, THP1 cells that were stably transfected with NLRP13 were treated with PMA and NLRP13 levels again decreased upon differentiation (Figure 5.14). Low Actin level of PMA differentiated cells is due to cell death during differentiation (approximately % 40).

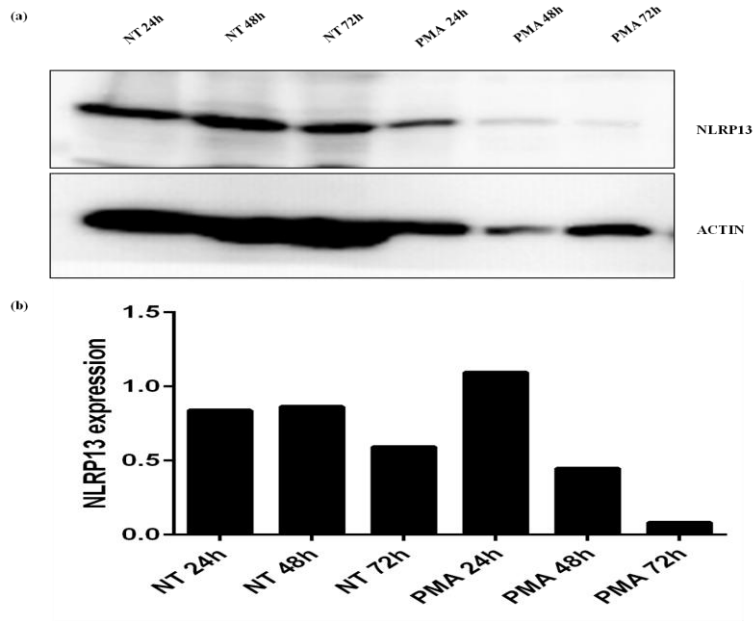

Figure 5.14. NLRP13 expression decreases during monocyte differentiation into macrophage. (a) NLRP13 levels were detected by WB. (b) NLRP13 was normalized to Actin.

Stably NLRP13 expressing THP1 cells were used in this experiment and it is expected that NLRP13 should be at a certain level and independent from transcriptional regulators of the host. This decrease should be result from post-transcriptional events. This data shows that NLRP13 is processed by post transcriptional events during macrophage differentiation.

5.6. NLRP13 is recruited to ASC specks

Under resting conditions, ASC is a cytoplasmic protein and it leads to the formation of speck-like structures with other inflammasome components during infection (Stutz *et al.*, 2013). Also, it was shown that NLRP13 interacts with ASC in HEK293FT cell in overexpression conditions.

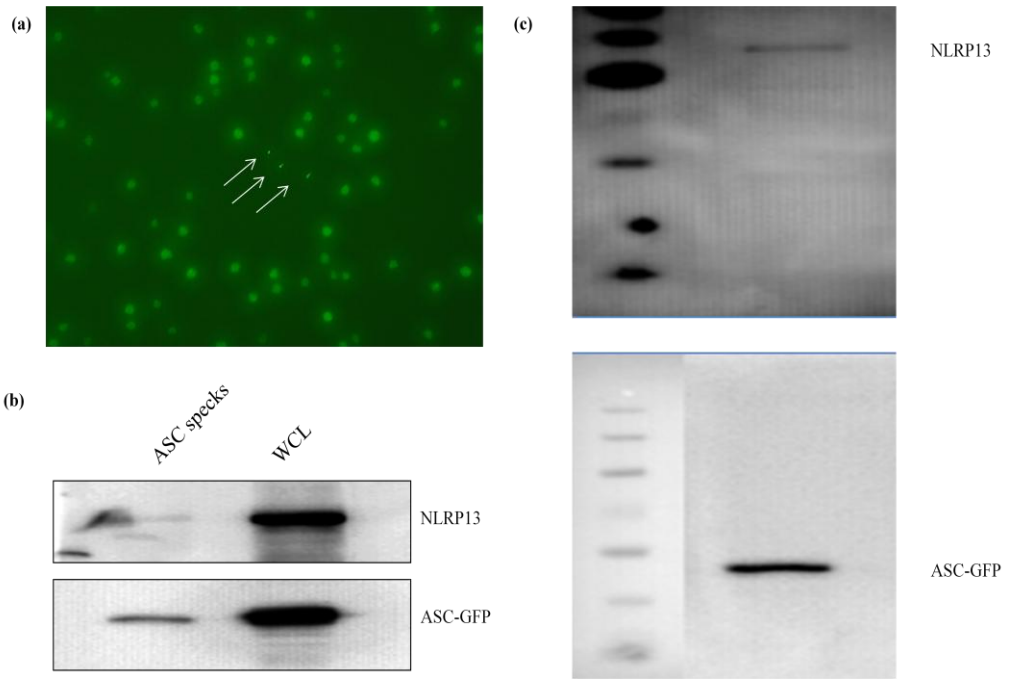

Figure 5.15. NLRP13 is recruited to ASC specks. (a) THP1-ASC-GFP and NLRP13 cells were treated with LPS and ATP. (b) ASC specks and NLRP13 were detected via WB (c) ASC specks were purified and NLRP13 and ASC levels were detected via WB.

To see whether NLRP13 is recruited to ASC specks during inflammasome formation, we created a stable THP-1 cell line, which expresses NLRP13 by lentiviral transduction. We already had THP1-ASC-GFP cells and NLRP13 was stably expressed in these cells for speck experiments. THP1 cells stably expressing ASC-GFP and NLRP13 were treated with LPS and ATP. LPS and ATP were chosen for treatment because it was shown that LPS and ATP are upstream regulators of NLRP13 during inflammation. Cells were observed under the inverted fluorescent microscope and the presence of ASC specks in some cells was confirmed. The arrows show the cells where ASC speck formed (Figure 5.15a). ASC specks were purified and it was shown that NLRP13 is recruited to the LPS-ATP dependant ASC specks (Figure 5.15).

5.7. NLRP13 Changes Inflammatory Cytokine Secretion

Inflammasomes are regulators of inflammatory responses where cytokine and chemokine expression and secretion are regulated by different inflammasomes in response to different pathogenic molecules. For example, NLRP3 inflammasome upregulates IL-1β, IL-18, IL-6 and TNF-α secretion (Schroder & Tschopp, 2010). We tried to see the effect of NLRP13 on inflammatory cytokines. To do this, THP1-NLRP13 cells were used and treated with LPS and ATP and then expression and secretion of cytokines were detected by WB for cytokine levels inside the cells and ELISA for secreted cytokines. THP1 control cells transduced with an empty plasmid were used as negative control. Mature IL-1β and proIL-1β levels were normalized to Actin levels. NLRP13 increased proIL-1β and mature IL-1β levels upon LPS and ATP treatment, on the other hand; secreted IL-1β was not affected significantly by NLRP13 (Figure 5.16). These results show that NLRP13 increases proIL-1β expression. The proIL-1β and mature IL-1β levels were increased due to the increase in proIL-1β expression.

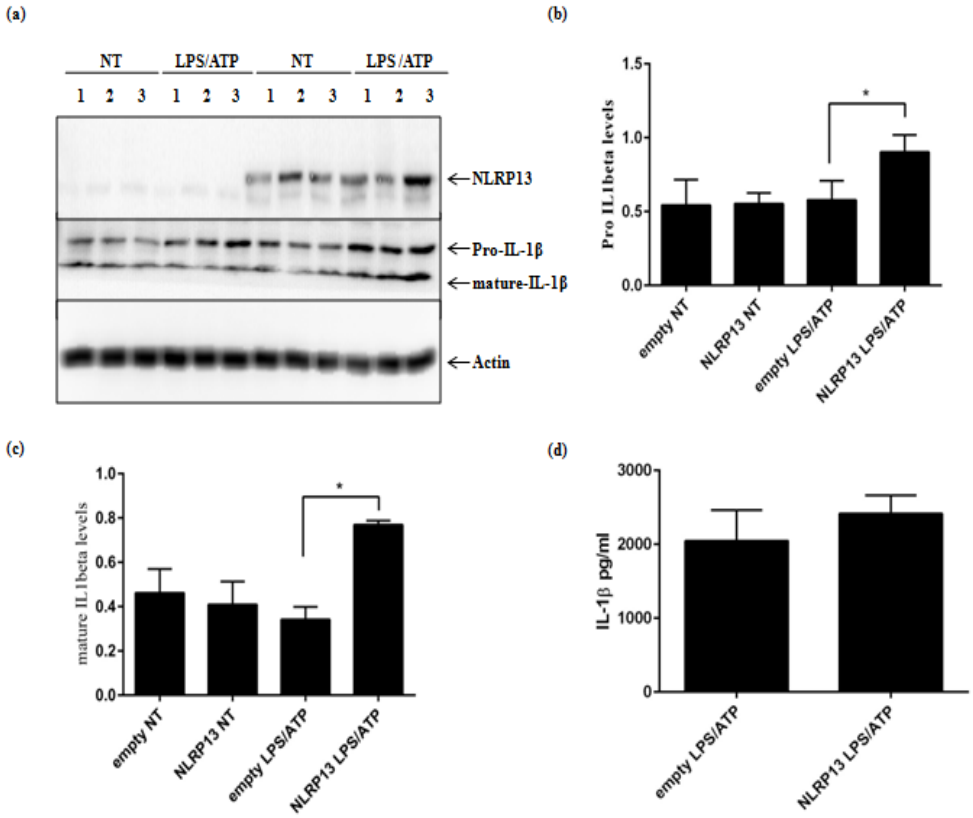

Figure 5.16. NLRP13 increases proIL-1β and mature IL-1β levels. (a) NLRP13, Actin and IL-1β levels were detected by WB. (b) ProIL-1β levels were analyzed by Image J. (c) Mature IL-1β levels were analyzed by Image J. (d) Secreted IL-1β levels were detected by ELISA.

Additionally, the effect of NLRP13 on TNF-α secretion was tested in THP1 macrophages upon LPS and ATP treatment, NLRP13 increased TNF-α secretion upon LPS and ATP treatment in THP1 macrophages.

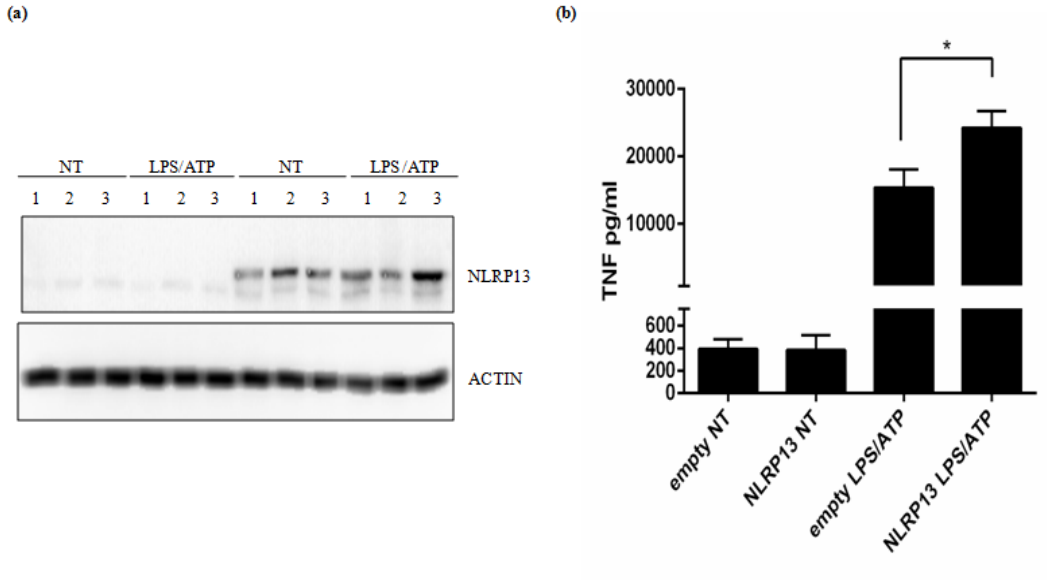

Figure 5.17. NLRP13 increases TNF-α secretion upon LPS and ATP treatment in THP1 macrophages. (a) NLRP13 levels were detected via WB. (b) TNF-α secretion was detected via ELISA.

Then, we wanted to see how secretions of other inflammatory cytokines and chemokines are affected by NLRP13. To do this, Human Inflammation Antibody Array which contains forty inflammatory cytokines was purchased. In this array, specific cytokine antibodies were conjugated to specific dots of the array membrane and a cocktail of biotin conjugated anti-cytokine antibodies was used to find specific cytokines on their dots. Finally, HRP-streptavidin was used to detect the cytokines by chemiluminescence via CCD cameras of Stella imaging system. We used THP1-NLRP13 and THP1 control cells in this experiment. These cells were differentiated with PMA as in previous experiments and then the cells were incubated 48 hours in cell culture conditions. After 48 hours, the cell supernatants of THP1-NLRP13 and THP1 control cells were collected and used in Inflammation Antibody Array. For analysis, fold change in cytokine secretions was calculated by normalizing THP1 NLRP13 cells' signal to THP1 control cells' signal (Figure 5.18).

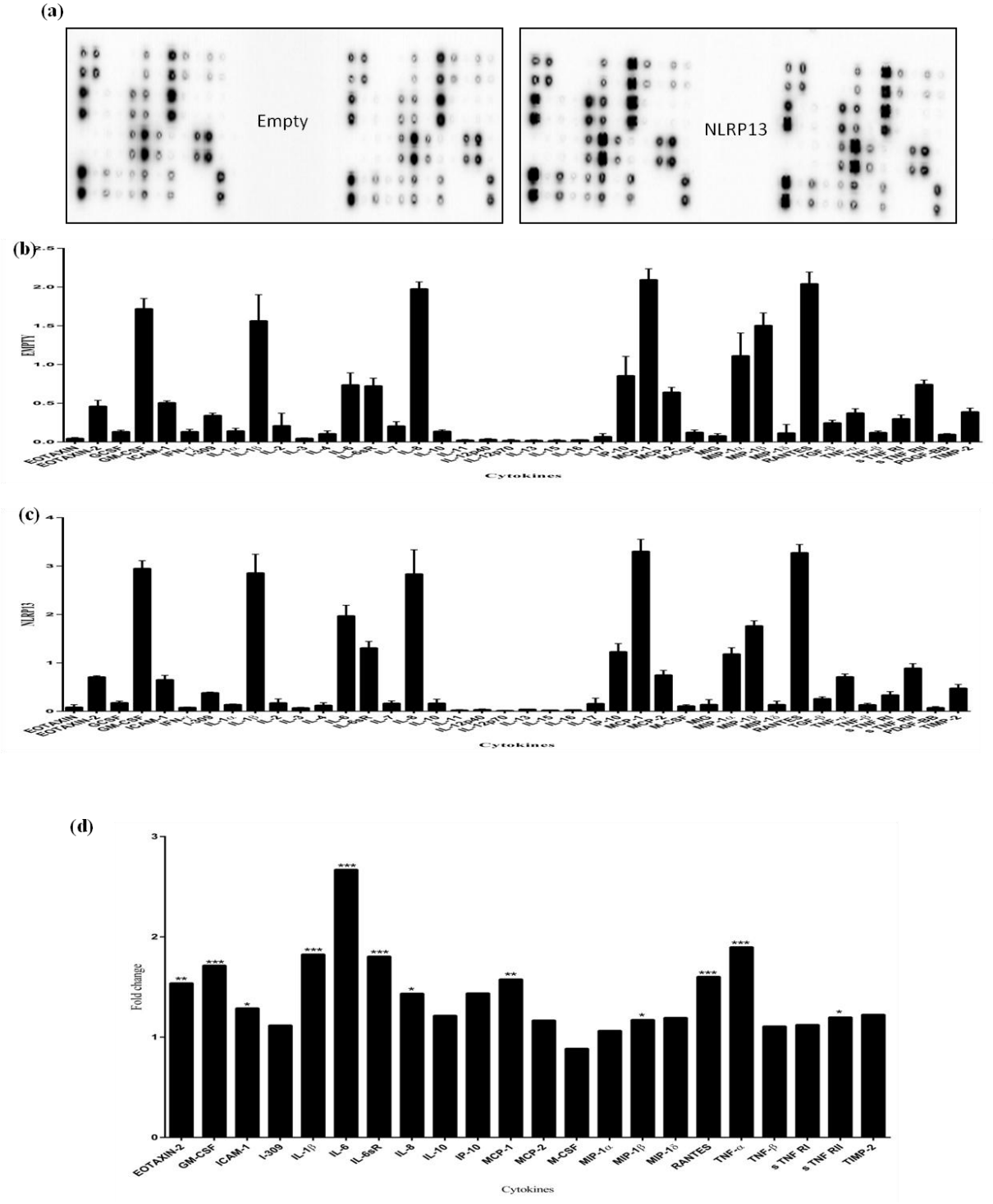

Figure 5.18. NLRP13 up-regulates secretions of pro-inflammatory cytokines. (a) Cytokines were detected via cytokine array by chemiluminescence via CCD cameras of Stella imaging system. (b) Cytokine profiling of THP1 empty cells (c) Cytokine profiling of THP1 NLRP13 cells (d) Fold change in cytokine secretions

As can be seen in the Figure 5.18; IL-6, IL-6Sr, IL-1β, GM-CSF, TNF-α and RANTES secretions increased in THP1-NLRP13 macrophages in comparison to THP1-control cells.

5.8. Study of Involvement of NLRP13 in Inflammation using Conditioned Medium System Mimicking Maternal-fetus Interphase

Our bioinformatic analysis showed that NLRP13 expression is very high in oocytes until blastocyst stage. So, we hypothesized that NLRP13 might have a role in early implantation during pregnancy. To figure out whether NLRP13 can affect inflammation through throphoblasts, NLRP13 was overexpressed in Swan71 throphoblast cells and the medium of these cells that were grown in low serum conditions was used to treat THP1 monocytes at different time points. Then, pro-IL-1β and mature IL-1β protein levels were tested via WB. There is a two fold increase in pro-IL-1β expression when THP1 cell were treated for 12 h with serum of Swan71-NLRP13 throphoblasts. For 24h treatment, there is a 1.6 fold increase in pro-IL-1β expression.

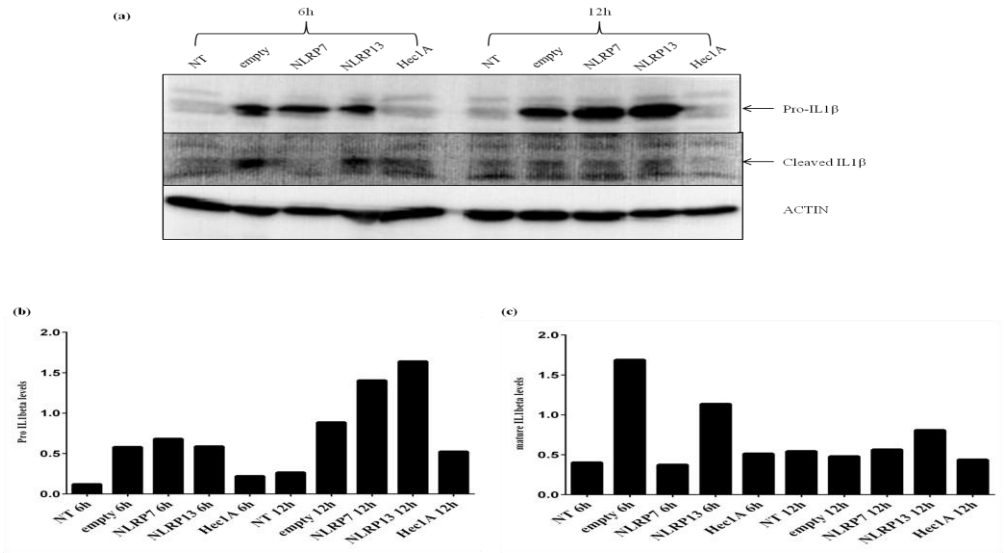

Figure 5.19. NLRP13 increases pro-IL-1β expression in THP1 cells upon education with conditioned medium from Swan71 throphoblasts. (a) IL-1β levels were detected via WB. (b) pro-IL-1β and mature pro-IL-1β levels were quantified using Image J.

When we look at the maturation of pro-IL-1β, it was seen that there is a 0.6 fold increase in mature IL-1β levels for 12h treatment. Also, differentiation of monocytes was observed upon treatment, such that the round floating monocytes started to attach to the plate.

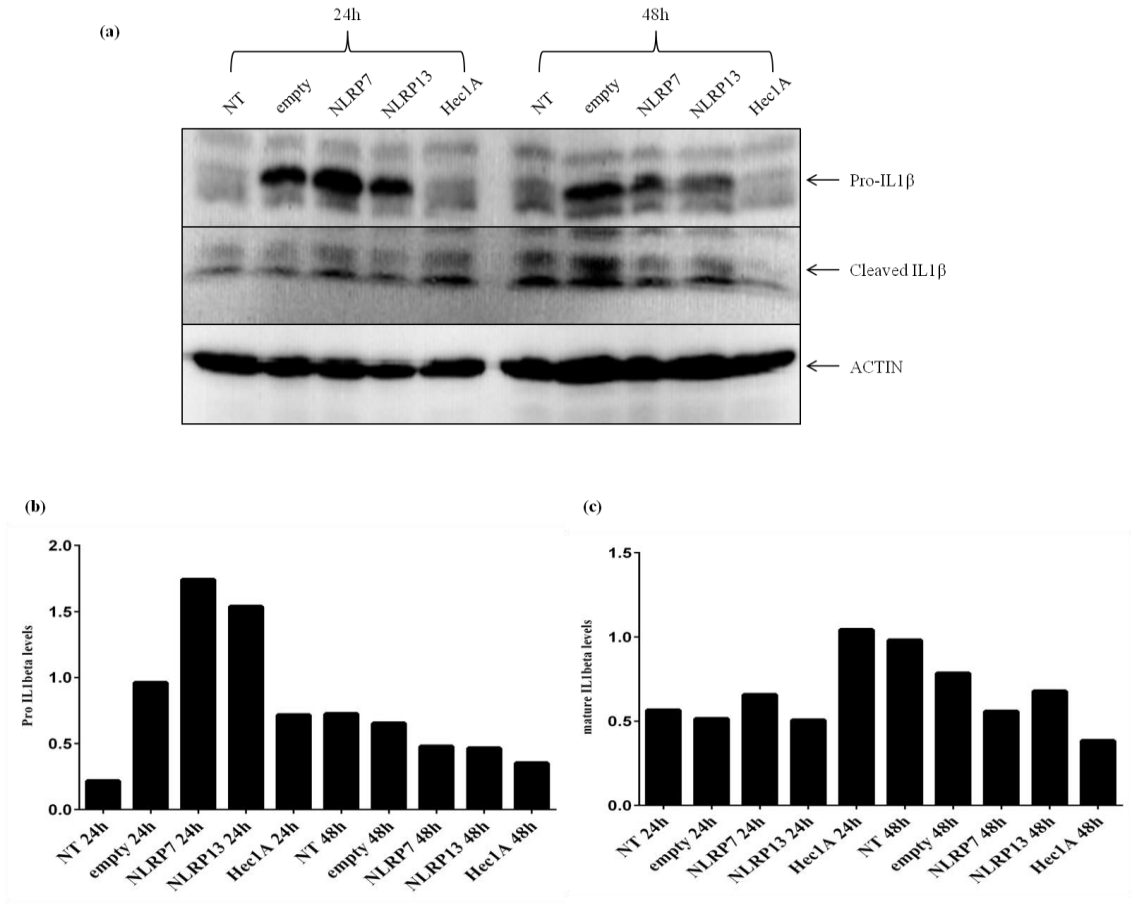

Figure 5.20. NLRP13 increases pro-IL-1β expression in THP1 cells after education with conditioned medium from Swan71 throphoblast. (a) IL-1β levels were detected via WB. (b) pro-IL-1β and mature pro-IL-1β levels were quantified using Image J.

Also, we investigated how IL-6 secretion in THP1 cells is affected by NLRP13 overexpression in Swan71 cells. To do this, IL-6 secretion was measured by ELISA and a slight increase was observed when THP1 cell were treated for 12 h and 24 h with conditioned medium of Swan71-NLRP13 throphoblasts. To conclude, NLRP13 does not have signicificant effect on IL-6 secretion in THP1 cells upon Swan-71 education.

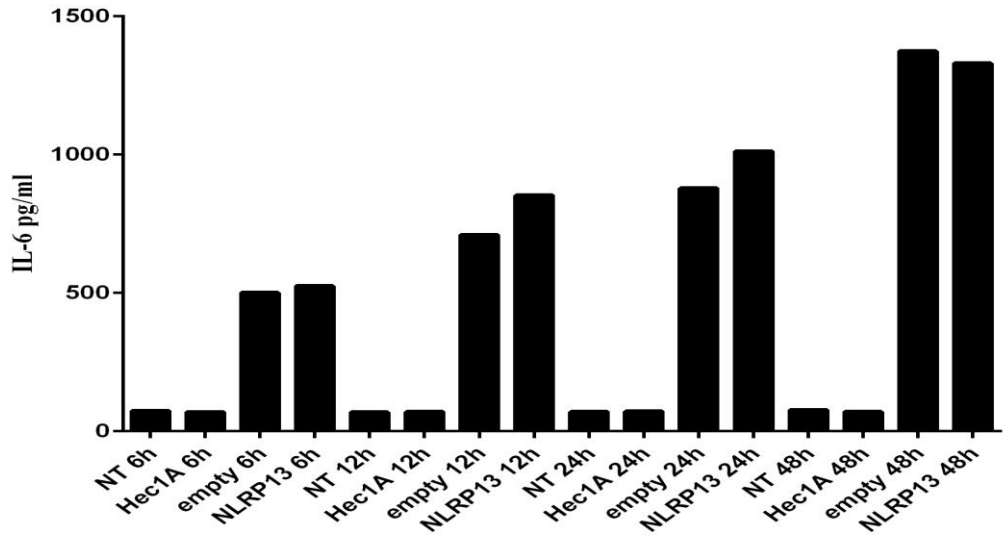

Figure 5.21. NLRP13 increases slighty IL-6 secretion in THP1 cells upon education with conditioned medium from Swan71 throphoblasts.

6. DISCUSSION

So far, no study about NLRP13's function is available in the literature besides the pioneering thesis of Yetiş Gültekin, (Gültekin, 2011) where he showed that NLRP13 is mainly localized in the cytoplasm and partially in mitochondria (% 35) using confocal microscopy. Also, he could show that NLRP13 weakly interacts with inflammatory proteins ASC and Caspase-1 but not with Caspase-5 in co-immunoprecipitation experiments. An inflammasome-like structure between ASC-Caspase-1 and NLRP13 was observed under overexpression conditions. Additionally, Gültekin showed that there is no significant effect of NLRP13 on ASC speck formation. In this study, we further characterized NLRP13 by investigating its role in inflammasome activity and immune regulation mechanisms. We firstly tried to find upstream regulators of NLRP13 during inflammasome activation. We showed that NRLP13 is recruited to ASC specks that formed dependant on LPS and ATP treatment. In addition, we analyzed which cytokine and chemokine secretions are regulated by NLRP13 after inflammatory stimulation. Finally, a possible role of NLRP13 in regulation of inflammation at the maternal-fetus interface during pregnancy was investigated because of high expression level of NLRP13 in oocytes and early embryos.

Because NLRP13 is an uncharacterized member of the NLR family, we thought that interaction partners of NLRP13 would help us put forward an idea about its function. For this purpose, we produced monoclonal and polyclonal anti-NLRP13 antibodies and mass spectrometry was done to identify NLRP13-related proteins after immunoprecipitation using these antibodies. Our antibodies worked well in Western Blotting experiments and overexpression conditions. Then, we looked at the NLRP13 expression in our cell lines. The monoclonal antibody (2C11) generated in this study recognized mostly a nearly 90 kDa protein in all cell lines except Raw macrophages. Additionally, a 38 kDa protein was detected in THP1 monocytes. This observation led to the idea that NLRP13 may be processed post-translationally or it may have shorter splice variants. To address these possibilities, we performed mass spectrometry analysis. First, NLRP13 was immunoprecipitated endogenously. Both polyclonal and monoclonal anti-

bodies were used for immunoprecipitation of NLRP13 in Swan71 cells. Because the same band was immunoprecipated by two different antibodies, these immunoprecipitation samples were analyzed using mass spectrometry analysis. Normally, high number of peptides should be obtained from immunoprecipitated protein and less number of peptides can be obtained from its possible interaction partners. However, there were only three peptides for NLRP13 in samples for which polyclonal Ab was used. This means that NLRP13 was precipitated in very low amount even if it was detected very well in Western Blotting. These unexpected results made it impossible to find interaction partners of our protein under endogenous conditions. From these results, it can be concluded that there is not enough NLRP13 expression in order to precipitate the protein in high amounts for mass spectrometry analysis in Swan71 cells and our antibodies mostly recognize and precipitate other proteins mostly in a nonspecific manner because other peptides were obtained in higher amounts than NLRP13 peptides. During immunoprecipitation experiments, attempts to knockdown NLRP13 by shRNA lentiviral transduction failed and we could not knockdown this 90 kDa protein. Then, we decided to overexpress NLRP13 in our cell lines for immunoprecipitation and other functional experiments. The monoclonal antibody 2C11 precipitated NLRP13 with correct size and high quantity in stably transfected Hec1A cells and these samples were used for mass spectrometry analysis. However, there were only four peptides for NLRP13 in our positive samples and we could not get any results from this analysis. Thus, we conclude that the monoclonal antibody does not work well in immunoprecipitation experiments. NLRP13 was injected to the mice and rabbits in denatured conditions and this can explain why our antibody recognizes linear forms of NLRP13 in WB, whereas it is unable to precipitate it in natural conditions. For these reasons, one could try to overexpress a tagged version of NLRP13 such as Flag and perform immunoprecipitations with an anti-Flag antibody for mass spectrometry analyses.

After detection of lower MW proteins during Western Blot analysis, we speculated that NLRP13 may be processed post-translationally. Also, there are putative caspase cleavage sites in the NLRP13 primary sequences. For this purpose, NLRP13 was co-transfected with different caspases in HEK 293FT cells and it was seen that NLR13 levels decreased sharply when cotransfected with Caspase 8 or 9. Then,

NLRP13 was cotransfected with Caspase 8, 9 or their mutant versions. In addition to decrease in full length of NLRP13 levels, a 38 kDa fragment was detected after cleavage of NLRP13 by Caspase 8 and 9. When we overexpressed only NLRP13, the lower 38 kDa band is also present but the intensity of the band increases when NLRP13 was cotransfected with Caspase-8 or 9. Possibly, endogenous Caspase 8 and 9 cleave NLRP13 up to some point but cleavage of NLRP13 increases during overexpression of the caspases. To see NLRP13 processing during apoptosis, NLRP13 overexpressing Tera-2 cells were treated with doxorubicin which activates the intrinsic apoptotic pathway and Caspase 9 after causing DNA damage. In non-treated Tera-2 cells, GFP-NLRP13 and lower 38 kDa band were detected but full form of NLRP13 was completely lost whereas lower 38 kDa band level sharply decreased. Caspase 8 and 9 are the initiator caspases of extrinsic and intrinsic apoptotic pathways, respectively and these caspases activate executioner caspases Caspase 3, 6 and 7 that can be responsible for further NLRP13 cleavage.

NLRs are cytoplasmic regulators of immune responses activated by pathogenic and danger signals. Some well-characterized members of the NLR family sense specific PAMPs and DAMPs, make its specific inflammasome with ASC and Caspase-1 and regulate cytokine and immune regulatory molecules to respond to their signals. To characterize NLRP13, we first tried to find which inflammatory molecules can be upstream regulators of NLRP13. Increase in NLRP13 expression upon a specific inflammatory molecule means that NLRP13 has a role in the immune response against this specific molecule. In our experiments, NLRP13 expression decreases upon LPS priming and subsequent ATP stimulation is the most potent second signal of NLRP13 because ATP increased NLRP13 expression by almost five-fold. ATP is present in every cell as energy source but extracellular ATP regulates other biological processes. Extracellular ATP functions as secondary messenger in inflammation and immune responses (Bours *et al*., 2006). For example, extracellular ATP activates NLRP3 inflammasome and promotes IL-1β and IL-18 maturation and release through P2X receptors which are cation-permeable ligand gated ion channels that open after ATP binding (Chen *et al*., 2013). For these reasons, LPS and ATP were used for the following experiments for further characterization of NLRP13.

After inflammasome activation, ASC assembles into large protein complexes called ASC specks. In each cell that forms an inflammasome, one ASC speck is observed. Different inflammatory proteins can get together into the speck depending on the signal. We showed that NLRP13 is recruited to ASC specks that formed upon LPS and ATP treatment of THP-1 stably NLRP13 and ASC-GFP. The recruitment of NLRP13 to the specks supports our previous data, where it was shown that there is weak interaction between NLRP13 and ASC and these two proteins co-localized in HEK293 FT cells under overexpression conditions (Gültekin, 2011).

NLRP13 increased proIL-1β and mature IL-1β levels upon LPS and ATP treatment, on the other hand; secreted IL- 1β was not affected by NLRP13 at the 3.5 hours time point. For fine-tuning of IL-1β secretion, IL-1β expression depending on the first signal, IL-1β maturation through inflammasome and secretion of IL-1β via secretory pathways should be regulated. In our experiments, IL-1β expression and maturation were increased upon NLRP13 overexpression but IL-1β secretion did not change significantly. Also, it was shown that NLRP13 increased TNF-α secretion upon LPS and ATP treatment in THP1 macrophages. TNF-α expression depends on the first signal of the inflammasome and TNF-α maturation is independent of the inflammasome based Caspase-1 cleavage. From these results, it can be concluded that NLRP13 somehow positively regulates NF-κB signaling to express more inflammatory cytokines but IL-1β secretion is unaffected and more detailed time course studies are needed whereas TNF-α secretion increased by NLRP13 although expression of both cytokines increased. These differences in changes of secretion may come from different secretory pathways used for secretion of different cytokines.

Interestingly, NLRP13 protein levels decreased about three fold during differentiation of monocytes to macrophages upon PMA treatment. From this observation, it can be speculated that NLRP13 may have a role in monocyte-macrophage transition. Similar results were seen when THP1 cells that stably express NLRP13 were treated with PMA. Again NLRP13 levels decreased upon differentiation. This decrease could result from post-transcription events. These results show that NLRP13 expression decreases after differentiation of monocytes into macrophages. Depending on the immune regulatory

molecules and microenvironment, monocytes are differentiated into different macrophage subtypes, mainly M1 and M2 macrophages. M1 macrophages are important for inflammation and anti-tumor activity and they secrete TNF-α, IL-6, IL-1β, RANTES, IP-10 and IL-12. M1 macrophages are activated by IFN-γ and LPS or TNFα. In contrast, M2 macrophages are characterized with their low IL-12 secretion and they contribute to wound healing and suppression of anti tumor activity. M2 macrophages are grouped into three subgroups: M2a, M2b and M2c macrophages. M2a macrophages are induced by IL-4 or IL-13 or IL-21; M2c macrophages are activated by TLR or IL-1 ligands; and M2cs are induced by IL-10 and TGF-β (Liu & Yang, 2013). Analysis of cytokine profile of macrophages after NLRP13 expresion it resembles mostly the cytokine profile of M1 macrophages. The most secreted cytokines are IL-6, IL-1β, GM-CSF, IL-8, IP-10, MIP1α, MIP1β and RANTES. When comparing THP1 NLRP13 cells to THP1 control cells in terms of cytokine secretions, IL-6, IL-6Sr, IL-1β, GM-CSF, IP-10, and TNF-α and RANTES secretions increased significantly in THP1-NLRP13 macrophages. Changes in these cytokines show that NLRP13 lead to differentiation of monocytes into more M1 macrophage subgroup and it can be said that NLRP13 promotes inflammation, host defense and anti-tumor activity. As mentioned before, M1 macrophages are activated by IFN-γ and LPS or TNFα. These M1 activators trigger different cell signaling pathways; IFN-γ activates STAT1 (signal transducers and activators of transcription 1) and interferon regulatory factors, such as IRF-1 and IRF-8 to control specific gene expression programs involving cytokine receptors and cell activation markers. LPS is another M1 macrophage signal and is a TLR4 ligand. After LPS stimulation of TLR4, MyD88 and MaL/Tirap-dependent pathways are activated and activation of these pathways leads to strong pro-inflammatory cytokines and chemokines that are controlled by NF-κB, activator protein 1 (AP-1), IRFs and STAT1 (Martinez & Gordon, 2014). Taken together our results, we suggest that NLRP13 somehow regulates these pathways and leads to differentiation of monocytes into macrophages of the M1 subgroup.

The inflammatory environment of the epithelium in the uterus is crucial for proper placentation during early phase of fetus-uterus implantation. Trophoblast cells of the placenta create this environment by secreting cytokines and chemokines for recruitment and differentiation of immune cells. Our bioinformatic analysis showed that NLRP13

expression is very high in oocytes and in early embryos until the blastocyst stage. We hypothesized that NLRP13 may play a role in early implantation. To test this hypothesis and figure out whether NLRP13 affects inflammation through throphoblast cells, NLRP13 was overexpressed in Swan71 throphoblast cells and the medium of these cells was used to treat THP1 monocytes at different time points. This treatment led to the differentiation of monocytes into macrophage-like cells and THP1 cells started to attach to the plate. The cytokine levels in THP1 cells showed a two fold increase in pro-IL-1β expression when THP1 cell were treated for 12 h with serum of Swan71-NLRP13 throphoblasts. After a 24h treatment, a 1.6 fold increase in pro-IL-1β expression was observed. Additionally, the maturation of pro-IL-1β showed a 0.6 fold increase in mature IL-1β levels after a 12h treatment. For the IL-6 case, a slight increase was observed when THP1 cell were treated with serum of Swan71-NLRP13 throphoblasts for 12 h and 24 h. As expected, NLRP13 appears to increase inflammation of monocytes through throphoblasts. To see the effect of NLRP13 on whole picture of inflammation, other cytokines should also be analyzed. Also, how other immune cells are affected in these interactions is another question that remains to be answered in the NLRP13- inflammation relationship at the maternal-fetus interface. Furthermore, MHC molecule expression, Fas-FasL and TRAIL-TRAIL receptor levels should be analyzed to see how these molecules are affected by NLRP13 in immune tolerance mechanisms during later stages of pregnancy.

Taking together our previous knowledge about NLRP13 and results obtained in this study, ATP and LPS appears to be upstream regulators of the NLRP13 inflammasome. NLRP13 forms an inflammasome-like structure with ASC and Caspase-1 and it is recruited to ASC specks after LPS and ATP treatment. NLRP13 increases TNF-α secretion and IL-1β expression upon ATP and LPS treatment. NLRP13 protein levels decrease upon both LPS priming and monocyte differentiation into macrophages by post-translational events, possibly by Caspase-8 initiated proteolytic digestion. Increase in IL-1β expression, not IL-1β secretion after NLRP13 stable expression shows that NLRP13 upregulates the NF-Kb signaling pathway and leads to increase in pro-inflammatory cytokine expression. Even if IL-1β expression increased, its secretion did not increase significantly because of NLRP13 does not have a role in processing of IL-

1β, which means that NLRP13 is not required for Caspase-1 activation and IL-1β cleavage although NLRP13 is recruited to ASC specks. Similar results were obtained from THP1 cells, which were educated with conditioned medium of NLRP13 expressing Swan71 throphoblasts in which NLRP13 increases IL-1β expression but IL-1β secretion does not change very much. Cytokine array results show that NLRP13 leads to differentiation of monocytes into macrophages of the M1subgroup and NLRP13 somehow regulates pathways that are important for differentiation, possibly through the NF-Kb signaling pathway.

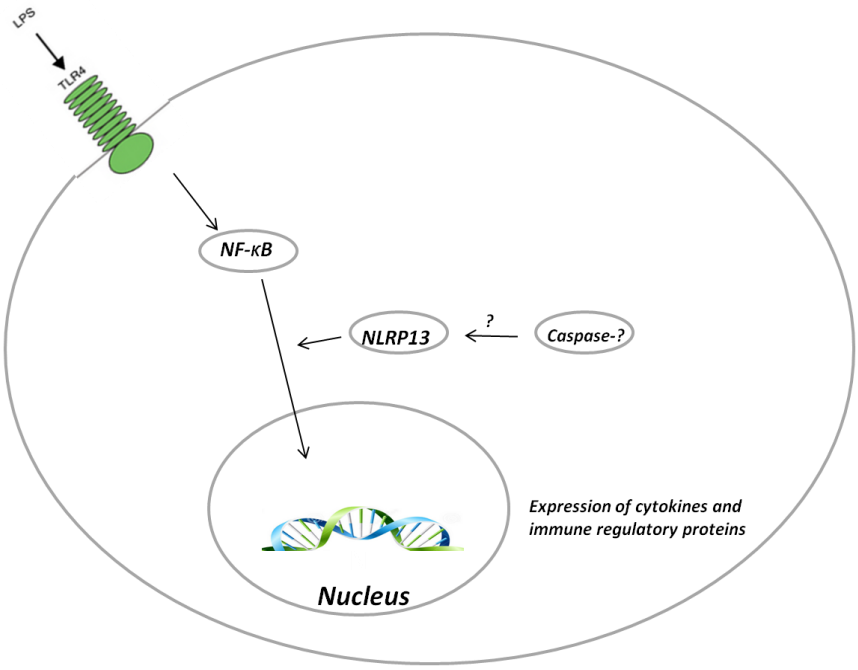

Figure 6.1. Our proposed model for NLRP13.

Based on our results, I propose that NLRP13 positively regulates the NF-Kb signaling pathway and leads to expression of inflammatory cytokine. In our model, Caspase-8 which also activates NF-Kb pathway cleaves NLRP13 and cleaved fragment of NLRP13 takes roles in expression of cytokines that are regulated by NF-Kb (Figure 6.1).

APPENDIX A: PLASMID MAPS

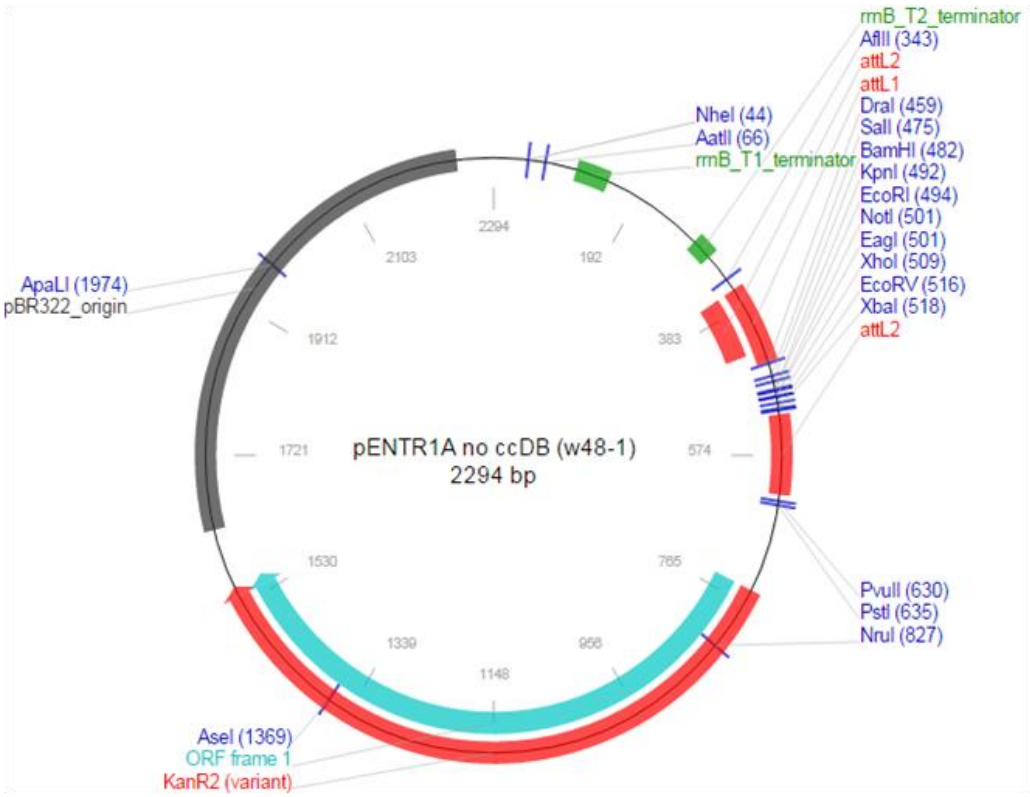

Figure A.1. Map of the pENTR1A donor vector.

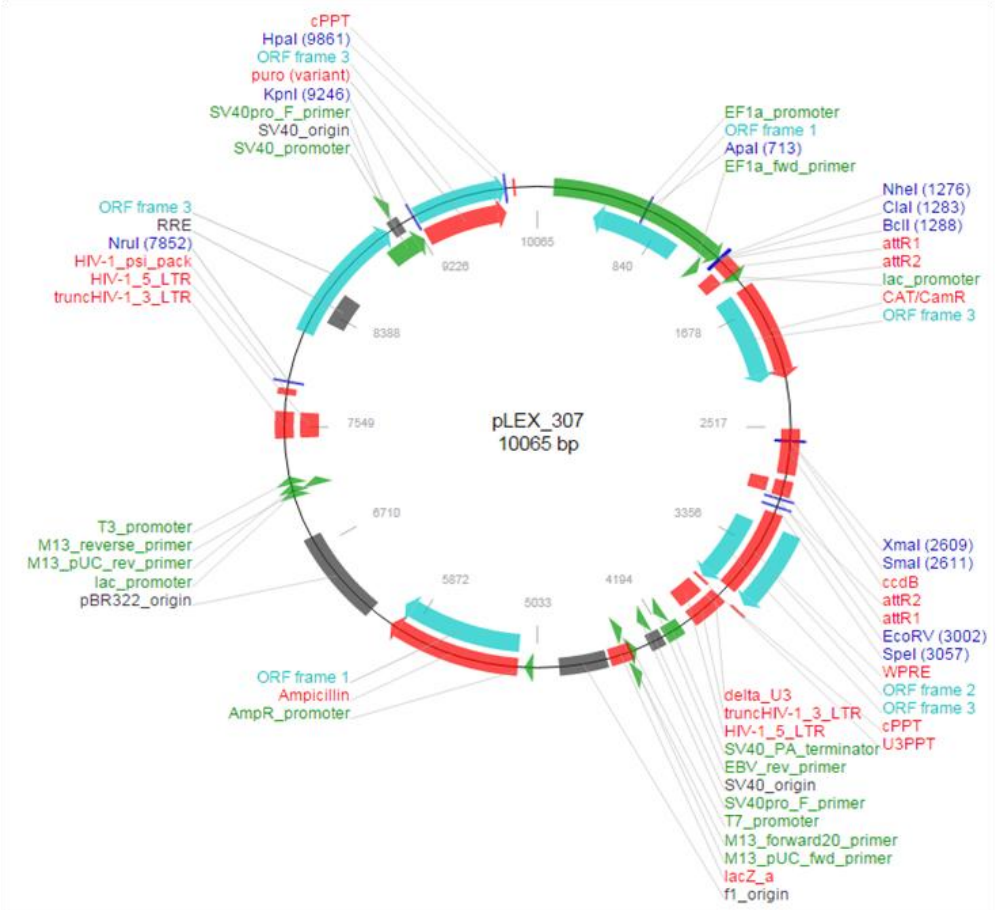

Figure A.2. Map of the pLex 307 lentiviral vector.

REFERENCES

Anand, P. K., R. K. Malireddi, and T. D. Kanneganti, 2011, "Role of the Nlrp3 Inflammasome in Microbial Infection", *Frontiers Microbiology*, Vol. 2, No., pp 12.

Antonopoulos, C., H. M. Russo, C. El Sanadi, B. N. Martin, X. Li, W. J. Kaiser, . . . G. R. Dubyak, 2015, "Caspase-8 as an Effector and Regulator of Nlrp3 Inflammasome Signaling", *The Journal of Biological Chemistry*, Vol. 290, No. 33, pp 20167-20184.

Barbe, F., T. Douglas, and M. Saleh, 2014, "Advances in Nod-Like Receptors (Nlr) Biology", *Cytokine Growth Factor Reviews*, Vol. 25, No. 6, pp 681-697.

Barker, C. F., and R. E. Billingham, 1977, "Immunologically Privileged Sites", *Advances in Immunology*, Vol. 25, No., pp 1-54.

Bergsbaken, T., S. L. Fink, and B. T. Cookson, 2009, "Pyroptosis: Host Cell Death and Inflammation", *Nature Reviews Microbiology*, Vol. 7, No. 2, pp 99-109.

Bours, M. J., E. L. Swennen, F. Di Virgilio, B. N. Cronstein, and P. C. Dagnelie, 2006, "Adenosine 5'-Triphosphate and Adenosine as Endogenous Signaling Molecules in Immunity and Inflammation", *Pharmacology and Therapeutics*, Vol. 112, No. 2, pp 358-404.

Chaudhary, P. M., M. T. Eby, A. Jasmin, A. Kumar, L. Liu, and L. Hood, 2000, "Activation of the Nf-Kappab Pathway by Caspase 8 and Its Homologs", *Oncogene*, Vol. 19, No. 39, pp 4451-4460.

Chen, K., J. Zhang, W. Zhang, J. Zhang, J. Yang, K. Li, and Y. He, 2013, "Atp-P2x4 Signaling Mediates Nlrp3 Inflammasome Activation: A Novel Pathway of

Diabetic Nephropathy", *The International Journal of Biochemistry and Cell Biology*, Vol. 45, No. 5, pp 932-943.

Fernandes, R., C. Tsuda, A. L. Perumalsamy, T. Naranian, J. Chong, B. M. Acton, . . . A. Jurisicova, 2012, "Nlrp5 Mediates Mitochondrial Function in Mouse Oocytes and Embryos", *Biology of Reproduction*, Vol. 86, No. 5, pp 138, 131-110.

Fink, S. L., and B. T. Cookson, 2005, "Apoptosis, Pyroptosis, and Necrosis: Mechanistic Description of Dead and Dying Eukaryotic Cells", *Infection and Immunity*, Vol. 73, No. 4, pp 1907-1916.

Fiszer, D., M. Ulbrecht, N. Fernandez, J. P. Johnson, E. H. Weiss, and M. Kurpisz, 1997, "Analysis of Hla Class Ib Gene Expression in Male Gametogenic Cells", *European Journal of Immunology*, Vol. 27, No. 7, pp 1691-1695.

Griffith, T. S., T. Brunner, S. M. Fletcher, D. R. Green, and T. A. Ferguson, 1995, "Fas Ligand-Induced Apoptosis as a Mechanism of Immune Privilege", *Science*, Vol. 270, No. 5239, pp 1189-1192.

Gültekin, Y., 2011, "*Cloning and Characterization of Novel Nod Like Receptors as Cytoplasmic Immune Sensors*", Master of Science, Bogazici University.

Hasegawa, M., Y. Fujimoto, P. C. Lucas, H. Nakano, K. Fukase, G. Nunez, and N. Inohara, 2008, "A Critical Role of Rick/Rip2 Polyubiquitination in Nod-Induced Nf-Kappab Activation", *EMBO Journal*, Vol. 27, No. 2, pp 373-383.

Huang, D. C., M. Hahne, M. Schroeter, K. Frei, A. Fontana, A. Villunger, . . . A. Strasser, 1999, "Activation of Fas by Fasl Induces Apoptosis by a Mechanism That Cannot Be Blocked by Bcl-2 or Bcl-X(L)", *Proceedings of the National Academy of Sciences USA*, Vol. 96, No. 26, pp 14871-14876.

Imamura, R., Y. Wang, T. Kinoshita, M. Suzuki, T. Noda, J. Sagara, . . . T. Suda, 2010, "Anti-Inflammatory Activity of Pynod and Its Mechanism in Humans and Mice", *Journal of Immunology*, Vol. 184, No. 10, pp 5874-5884.

Lamkanfi, M., and V. M. Dixit, 2014, "Mechanisms and Functions of Inflammasomes", *Cell*, Vol. 157, No. 5, pp 1013-1022.

Latz, E., A. Schoenemeyer, A. Visintin, K. A. Fitzgerald, B. G. Monks, C. F. Knetter, . . . D. T. Golenbock, 2004, "Tlr9 Signals after Translocating from the Er to Cpg DNA in the Lysosome", *Nature Immunology*, Vol. 5, No. 2, pp 190-198.

Lin, K. M., W. Hu, T. D. Troutman, M. Jennings, T. Brewer, X. Li, . . . C. Pasare, 2014, "Irak-1 Bypasses Priming and Directly Links Tlrs to Rapid Nlrp3 Inflammasome Activation", *Proceedings of the National Academy of Sciences USA*, Vol. 111, No. 2, pp 775-780.

Liu, G., and H. Yang, 2013, "Modulation of Macrophage Activation and Programming in Immunity", *Journal of Cell Physiology*, Vol. 228, No. 3, pp 502-512.

Martinez, F. O., and S. Gordon, 2014, "The M1 and M2 Paradigm of Macrophage Activation: Time for Reassessment", *F1000Prime Reports*, Vol. 6, No., pp 13.

Mellor, A. L., and D. H. Munn, 2004, "Ido Expression by Dendritic Cells: Tolerance and Tryptophan Catabolism", *Nature Reviews Immunology*, Vol. 4, No. 10, pp 762-774.

Meyer, E., D. Lim, S. Pasha, L. J. Tee, F. Rahman, J. R. Yates, . . . E. R. Maher, 2009, "Germline Mutation in Nlrp2 (Nalp2) in a Familial Imprinting Disorder (Beckwith-Wiedemann Syndrome)", *PLOS Genetics*, Vol. 5, No. 3, pp e1000423.

Mor, G., I. Cardenas, V. Abrahams, and S. Guller, 2011, "Inflammation and Pregnancy: The Role of the Immune System at the Implantation Site", *Annals New York Academy of Sciences*, Vol. 1221, No., pp 80-87.

Moresco, E. M., D. LaVine, and B. Beutler, 2011, "Toll-Like Receptors", *Current Biology*, Vol. 21, No. 13, pp R488-493.

Niederkorn, J. Y., 2006, "See No Evil, Hear No Evil, Do No Evil: The Lessons of Immune Privilege", *Nature Immunology*, Vol. 7, No. 4, pp 354-359.

Radian, A. D., L. de Almeida, A. Dorfleutner, and C. Stehlik, 2013, "Nlrp7 and Related Inflammasome Activating Pattern Recognition Receptors and Their Function in Host Defense and Disease", *Microbes and Infection*, Vol. 15, No. 8-9, pp 630-639.

Ramhorst, R., L. Fraccaroli, P. Aldo, A. B. Alvero, I. Cardenas, C. P. Leiros, and G. Mor, 2012, "Modulation and Recruitment of Inducible Regulatory T Cells by First Trimester Trophoblast Cells", *American Journal of Reproductive Immunology*, Vol. 67, No. 1, pp 17-27.

Ryan, A. F., R. L. Grendell, D. E. Geraghty, and T. G. Golos, 2002, "A Soluble Isoform of the Rhesus Monkey Nonclassical Mhc Class I Molecule Mamu-Ag Is Expressed in the Placenta and the Testis", *Journal of Immunology*, Vol. 169, No. 2, pp 673-683.

Sagulenko, V., S. J. Thygesen, D. P. Sester, A. Idris, J. A. Cridland, P. R. Vajjhala, . . . K. J. Stacey, 2013, "Aim2 and Nlrp3 Inflammasomes Activate Both Apoptotic and Pyroptotic Death Pathways Via Asc", *Cell Death and Differentiation*, Vol. 20, No. 9, pp 1149-1160.

Schneider, M., A. G. Zimmermann, R. A. Roberts, L. Zhang, K. V. Swanson, H. Wen, . . . J. P. Ting, 2012, "The Innate Immune Sensor Nlrc3 Attenuates Toll-Like Receptor Signaling Via Modification of the Signaling Adaptor Traf6 and Transcription Factor Nf-Kappab", *Nature Immunology*, Vol. 13, No. 9, pp 823-831.

Schroder, K., and J. Tschopp, 2010, "The Inflammasomes", *Cell*, Vol. 140, No. 6, pp 821-832.

Streilein, J. W., 2003, "Ocular Immune Privilege: Therapeutic Opportunities from an Experiment of Nature", *Nat Reviews Immunology*, Vol. 3, No. 11, pp 879-889.

Stutz, A., G. L. Horvath, B. G. Monks, and E. Latz, 2013, "Asc Speck Formation as a Readout for Inflammasome Activation", *Methods in Molecular Biology*, Vol. 1040, No., pp 91-101.

Takeuchi, O., and S. Akira, 2010, "Pattern Recognition Receptors and Inflammation", *Cell*, Vol. 140, No. 6, pp 805-820.

Thompson, M. R., J. J. Kaminski, E. A. Kurt-Jones, and K. A. Fitzgerald, 2011, "Pattern Recognition Receptors and the Innate Immune Response to Viral Infection", *Viruses*, Vol. 3, No. 6, pp 920-940.

Wang, S., and W. S. El-Deiry, 2003, "Trail and Apoptosis Induction by Tnf-Family Death Receptors", *Oncogene*, Vol. 22, No. 53, pp 8628-8633.

Zhang, P., M. Dixon, M. Zucchelli, F. Hambiliki, L. Levkov, O. Hovatta, and J. Kere, 2008, "Expression Analysis of the Nlrp Gene Family Suggests a Role in Human Preimplantation Development", *PLOS One*, Vol. 3, No. 7, pp e2755.